Smaug1 mRNA-silencing foci respond to NMDA and modulate synapse formation

María Verónica Baez,[1,2] Luciana Luchelli,[1,2,3] Darío Maschi,[1,2,3] Martín Habif,[1,3] Malena Pascual,[1,2,3] María Gabriela Thomas,[1,2] and Graciela Lidia Boccaccio[1,2,3]

[1]Fundación Instituto Leloir, C1405BWE Buenos Aires, Argentina
[2]Instituto de Investigaciones Bioquímicas Buenos Aires-Consejo Nacional de Investigaciones Científicas y Tecnológicas, C1405BWE Buenos Aires, Argentina
[3]Facultad de Ciencias Exactas y Naturales, University of Buenos Aires, C1428EHA Buenos Aires, Argentina

Mammalian Smaug1/Samd4A is a translational repressor. Here we show that Smaug1 forms mRNA-silencing foci located at postsynapses of hippocampal neurons. These structures, which we have named S-foci, are distinct from P-bodies, stress granules, or other neuronal RNA granules hitherto described, and are the first described mRNA-silencing foci specific to neurons. RNA binding was not required for aggregation, which indicates that S-foci formation is not a consequence of mRNA silencing. *N*-methyl-D-aspartic acid (NMDA) receptor stimulation provoked a rapid and reversible disassembly of S-foci, transiently releasing transcripts (the CaMKIIα mRNA among others) to allow their translation. Simultaneously, NMDA triggered global translational silencing, which suggests the specific activation of Smaug1-repressed transcripts. Smaug1 is expressed during synaptogenesis, and Smaug1 knockdown affected the number and size of synapses, and also provoked an impaired response to repetitive depolarizing stimuli, as indicated by a reduced induction of Arc/Arg3.1. Our results suggest that S-foci control local translation, specifically responding to NMDA receptor stimulation and affecting synaptic plasticity.

Introduction

Local translation at the synapse is an important mechanism for synaptic plasticity. Hundreds of mRNAs encoding signaling molecules, channels, neurotransmitter receptors, and components and regulators of the actin cytoskeleton, among other cellular functions, are selectively transported to distinct dendritic domains. There, their translation and stability is closely regulated upon stimulation by specific neurotransmitters or trophic factors by several RNA binding proteins (RBPs) and microRNAs. Deregulation of local translation compromises synapse formation and function, and provokes a plethora of neurological disorders. The human condition fragile X mental retardation syndrome is a dramatic example (Steward et al., 1998; Wu et al., 1998, 2005; Scheetz et al., 2000; Aakalu et al., 2001; Steward and Worley, 2001; Ostroff et al., 2002; Dubnau et al., 2003; Eom et al., 2003; Zalfa et al., 2003, 2006, 2007; Antar et al., 2004; Atkins et al., 2004; Kelleher et al., 2004; Sutton et al., 2004; Bagni and Greenough, 2005; Du and Richter, 2005; Fujii et al., 2005; Shiina et al., 2005, 2010; Ashraf et al., 2006; Goetze et al., 2006; Poon et al., 2006; Schratt et al., 2006; Sutton and Schuman, 2006; Vessey et al., 2006, 2008, 2010; Bramham and Wells, 2007; Giorgi et al., 2007; Muddashetty et al., 2007; Dictenberg et al., 2008; Costa-Mattioli et al., 2009; Fiore et al., 2009; Holt and Bullock, 2009; Martin and Ephrussi, 2009; De Rubeis and Bagni, 2010; Dieterich et al., 2010; Hillebrand et al., 2010). Localized mRNAs are found in granules, collectively known as neuronal RNA granules, that contain specific RBPs including Staufen 1 and 2, Pumilio, fragile X mental retardation protein (FMRP), RNA granule protein 105 (RNG105), zipcode-binding protein 1 (ZBP1), survival of motor neuron

M.V. Baez, L. Luchelli, and D. Maschi contributed equally to this paper.

Correspondence to Graciela Lidia Boccaccio: gboccaccio@leloir.org.ar

Dr. Colman died on 1 June 2011.

Abbreviations used in this paper: AHA, azidohomoalanine; AMPA, α-amino-3-hydroxy-5-methyl-4-isoxazolepropionic acid; AMPAR, AMPA receptor; Arc/Arg3.1, activity-regulated cytoskeletal-associated protein; CaMKII, Ca^{2+}/CaM-dependent protein kinase II; DCP1a, decapping enzyme 1a; FMRP, fragile X mental retardation protein; FUNCAT, fluorescent noncanonical amino acid tagging; GABA, γ-amino butyric acid; HPG, homopropargylglycine; IF, immunofluorescence; NB, Neurobasal medium; NMDA, *N*-methyl-D-aspartic acid; NMDAR, NMDA receptor; PB, processing body; PI3K, phosphoinositide 3-kinase; RBP, RNA binding protein; SG, stress granule; SRE, Smaug recognition element; TTX, tetrodotoxin; UTR, untranslated region.

The Rockefeller University Press $30.00
J. Cell Biol. Vol. 195 No. 7 1141–1157
www.jcb.org/cgi/doi/10.1083/jcb.201108159

(SMN), 4AIII, fused/translocated in sarcoma (FUS/TLS), and TAR DNA-binding protein 43 (TDP43), among others. Neuronal RNA granules serve as the functional units for transport and translational control (Knowles et al., 1996; Köhrmann et al., 1999; Steward and Worley, 2001; Kanai et al., 2004; Antar et al., 2004; Fujii et al., 2005; Shiina et al., 2005; Wu et al., 2005; Barbee et al., 2006; Schratt et al., 2006; Vessey et al., 2006; Giorgi et al., 2007; Bramham et al., 2008; Wang et al., 2008; Falley et al., 2009; Martin and Ephrussi, 2009; Thomas et al., 2011). In addition to neuronal RNA granules, the somatodendritic compartment contains processing bodies (PBs). PBs are ubiquitous mRNA-silencing foci, and they harbor untranslated mRNAs that can be released to allow translation. A plethora of PBs that differ subtly on composition are present in mammalian and insect neurons, and remarkably, neuronal PBs were recently shown to respond to synaptic stimulation (Barbee et al., 2006; Cougot et al., 2008; Savas et al., 2008; Zeitelhofer et al., 2008; di Penta et al., 2009; Miller et al., 2009; Thomas et al., 2011). Finally, stress granules (SGs), which are ubiquitous mRNA-silencing foci specific to the stress response, transiently form in neurons exposed to a variety of noxious stimuli. Several RBPs present in neuronal RNA granules are recruited to SGs, where they regulate mRNA translation, aggregation, and molecular motor recruitment (Thomas et al., 2005, 2009; Shiina et al., 2005; Vessey et al., 2006; Didiot et al., 2009; Loschi et al., 2009; Bosco et al., 2010; Liu-Yesucevitz et al., 2010).

In this paper, we investigated the relevance of mammalian Smaug1/Samd4A, a posttranscriptional regulator that belongs to a novel family of RBPs (Aviv et al., 2003), in translational regulation at the synapse. Smaug was initially described in *Drosophila melanogaster*. In this organism, Smaug controls the stability and translation of hundreds of maternal mRNAs during early development (Smibert et al., 1996; Dahanukar et al., 1999; Smibert et al., 1999; Nelson et al., 2004; Semotok et al., 2005, 2008; Tadros et al., 2007; Benoit et al., 2009). *Drosophila* Smaug mediates mRNA silencing by multiple mechanisms. One of them involves the recruitment of Cup, which binds eukaryote initiation factor 4E, thus interrupting its interaction with eukaryote initiation factor 4G and blocking translation initiation (Nelson et al., 2004). More recently, fly Smaug was shown to block cap-dependent and independent translation by forming a highly stable repressed messenger RNP (Jeske et al., 2011). *Drosophila* Smaug is also able to trigger deadenylation by recruiting the CCR4–NOT complex and specific Piwi-interacting RNAs (Zaessinger et al., 2006; Semotok et al., 2008; Rouget et al., 2010). The yeast homologue Vts1 similarly triggers deadenylation of target mRNAs by recruiting the CCR4–NOT complex (Rendl et al., 2008). Two homologous genes, Smaug1/Samd4A and Smaug 2, are present in the mammalian genome. In a previous study, we reported that mammalian Smaug1 is present in the central nervous system and absent from nonneuronal cell lines (Baez and Boccaccio, 2005). Mammalian Smaug1 represses the translation of mRNAs carrying a specific motif termed Smaug recognition element (SRE), which mediates the binding of the *Drosophila* and yeast molecules to their targets (Smibert et al., 1996; Dahanukar et al., 1999; Smibert et al., 1999; Crucs et al., 2000; Aviv et al., 2003, 2006; Green et al., 2003; Forrest et al., 2004; Semotok et al., 2005; Johnson and Donaldson, 2006; Oberstrass et al., 2006; Zaessinger et al., 2006; Tadros et al., 2007; Semotok et al., 2008; Foat and Stormo, 2009; Li et al., 2010; Ravindranathan et al., 2010). Here we found that Smaug1 forms granules in mature hippocampal neurons, which we have named S-foci, as they are apparently distinct from previously described neuronal RNA granules, as well as from PBs and SGs. S-foci are located at dendritic spines and behave as mRNA-silencing foci, being enhanced upon polysome breakdown, and disrupted upon polysome stabilization. We found that the Smaug1 RNA-binding domain is dispensable for S-foci formation, which indicates that Smaug1 aggregation is not the consequence of the binding to repressed mRNAs. Importantly, S-foci respond to synaptic stimulation, specifically to *N*-methyl-D-aspartic acid (NMDA) receptor (NMDAR) activation, which provokes the dissolution of the S-foci and the release of transcripts to allow their translation. We found that the messenger encoding the key molecule Ca^{2+}/CaM-dependent protein kinase II (CaMKIIα) is apparently regulated by this novel mechanism. Unlike most RBP components of neuronal granules, which are also present in nonneural cells, Smaug1 is neuron-specific and its expression is triggered during synaptogenesis. Remarkably, we found that Smaug1 knockdown provokes the formation of smaller and more numerous synapses. Moreover, Smaug1-depleted neurons respond defectively to a repetitive depolarizing stimulus, as indicated by a reduced induction of activity-regulated cytoskeletal-associated protein (Arc/Arg3.1), an activity marker gene. Our results suggest that Smaug1 regulates localized translation upon synaptic stimulation, thus affecting synapse biogenesis and/or stability.

Results

Smaug1 forms mRNA-silencing foci in cultured neurons

Having demonstrating the expression of Smaug1 in the central nervous system (Baez and Boccaccio, 2005), we analyzed the distribution of mammalian Smaug1 in mature neurons by immunofluorescence (IF). We found that Smaug1 forms granules ~0.5 µm in diameter, which were present in the cell body and dendrites (Fig. 1 A). Smaug1 granules were distinct from those containing FMRP, an RBP involved in mRNA regulation (Fig. 1 B; Bagni and Greenough, 2005; Dictenberg et al., 2008). As expected, primary fibroblasts and glial cells did not express Smaug1 (unpublished data; Baez and Boccaccio, 2005).

We have shown before that Smaug1 constructs transfected in nonneuronal cell lines form RNA granules that behave as silencing foci, as they are in dynamic equilibrium with translating polysomes (Baez and Boccaccio, 2005). We investigated whether neuronal Smaug1 foci behave similarly. We focused on dendritic granules, as the abundance of Smaug1 granules at the cell body precluded the analysis in this cell compartment. We found that a relatively long-exposure of cultured neurons to puromycin, a translation inhibitor that disrupts polysomes, enhanced the presence of Smaug1 granules, whereas cycloheximide, a drug that blocks elongation leading to ribosome stalling, provoked a moderate dissolution (Fig. 1 C). Shorter treatments

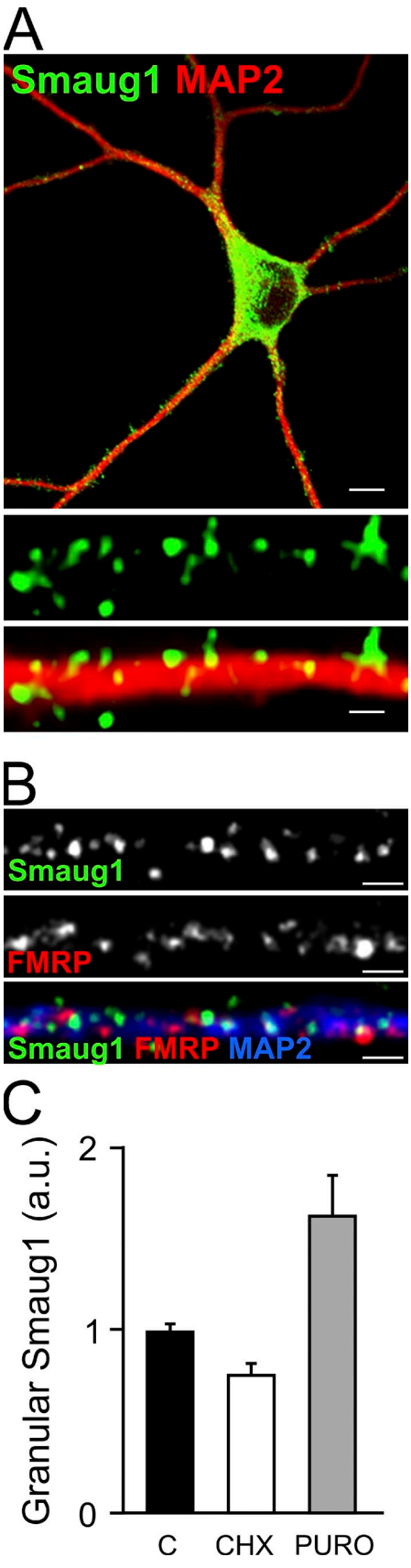

Figure 1. **Mammalian Smaug1 is expressed in neurons and forms mRNA-silencing foci.** Cultured hippocampal neurons were stained for the indicated molecules. (A) Bars: (top) 5 µm; (bottom) 1 µm. (B) A magnification of an isolated dendrite is shown. Bar, 1 µm. (C) Hippocampal neurons were exposed to cycloheximide (CHX) or puromycin (PURO) during 3 h. The size and number of Smaug1 foci were measure in 100× confocal z-stack images and the area occupied by Smaug1 granules in 20 randomly selected dendrite fragments was calculated for each treatment. A moderate increase of Smaug1 granular signal was observed upon puromycin treatment, whereas exposure to cycloheximide provokes a moderate reduction of Smaug1 granular signal. Error bars indicate standard deviation.

had no effect (see Fig. 6). For comparison, the dynamics of neuronal PBs identified by decapping enzyme 1a (DCP1a) staining were similarly analyzed. We found that PBs dissolved faster than Smaug1 foci upon polysome stabilization (unpublished data). These observations are consistent with the behavior of PBs in nonneuronal cells (for reviews see Franks and Lykke-Andersen, 2008; Anderson and Kedersha, 2009; Balagopal and Parker, 2009; Buchan and Parker, 2009; Kulkarni et al., 2010; Thomas et al., 2011). Thus, dendritic Smaug1 granules behave as mRNA-silencing foci, and are apparently less dynamic than PBs. We named structures that contain Smaug1; exclude FMRP, SMN, and Staufen 1 (Fig. 1; unpublished data); and are distinct from PBs and SGs (see the following section) "S-foci."

Smaug1 foci are independent of PBs

We investigated the relationship between S-foci and SGs and PBs. Neuronal S-foci appeared distinct from SGs formed upon exposure of neurons to an oxidative stress stimulus, but they were frequently found in the vicinity of SGs, thus resembling the behavior of PBs (Fig. S1 A). In contrast, FMRP and Staufen were recruited to SGs, as described previously in neuronal and nonneuronal cells (Fig. S1 A; Thomas et al., 2005, 2009; Didiot et al., 2009; Martinez Tosar et al., 2011). We then analyzed the relationship between S-foci and PBs by visualizing DCP1a. We found that neuronal S-foci did not overlap with PBs identified by DCP1a. However, a significant proportion of the S-foci were detected in close contact with PBs (Fig. S1 B). Next, we investigated whether PBs are required for S-foci formation. We treated neurons with siRNAs against the PB components Hedls, Rck/p54, or 4ET, which are known to affect PB integrity in cell lines (Fenger-Grøn et al., 2005; Ferraiuolo et al., 2005; Thomas et al., 2009). We found that the numbers of DCP1a foci were reduced upon depletion of any of the above molecules (Fig. 2 A), as reported recently in *Drosophila* neurons upon depletion of Rck/p54/Me31B (Hillebrand et al., 2010). We simultaneously analyzed the presence of the S-foci and found that their number or size were not affected by any of the treatments against PBs (Fig. 2 A). Conversely, Smaug1 depletion did not significantly affect the presence of PBs identified by DCP1a staining (Fig. S1 C). Collectively, these results indicate that PB integrity is not required for S-foci maintenance. However, the possibility that the S-foci were assembled before PB breakdown remained open. To investigate this, we used U2OS cells, which do not express Smaug1 (Baez and Boccaccio, 2005). As expected, transfected Smaug1-ECFP form cytoplasmic granules in U2OS (Fig. 2, A–C). Overexpression may provoke the formation of unfolded protein aggregates, and we considered this possibility. As described previously (Baez and Boccaccio, 2005), we found that Smaug1-ECFP foci are dynamic and behave as

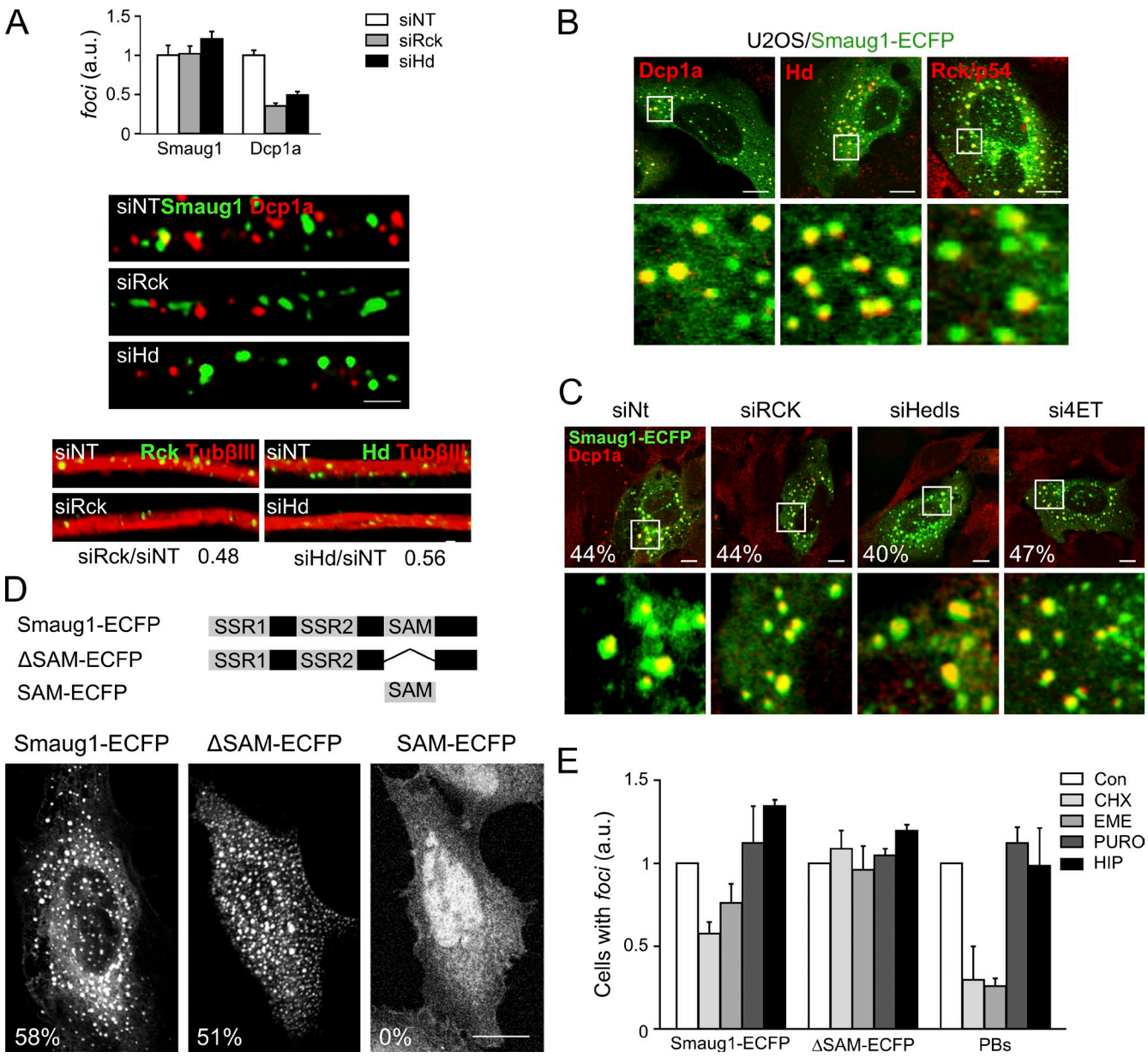

Figure 2. **S-foci are independent of PBs.** (A) Neurons were treated with the indicated siRNA, and the presence of S-foci and PBs visualized by DCP1a staining was analyzed in 20 randomly selected dendrite fragments (400 µm total length) for each treatment. Normalized values from two independent experiments are plotted. Representative IF images for the indicated molecules upon the distinct treatments are shown. Bottom, depletion of PBs visualized by RCK or Hedls relative to normal levels. In all cases, knockdown of Hedls or RCK provokes PB disruption without affecting the presence of S-foci. Error bars indicate standard deviation. (B) U2OS cells were transfected with Smaug1-ECFP and immunostained for the indicated PB markers. Close vicinity between S-foci and PBs is frequent (Fig. S2 A). The bottom row shows enlarged views of the boxed regions. (C) U2OS cells were treated with the indicated siRNAs, then transfected with the Smaug1-ECFP construct, and stained for DCP1a. Depletion of Hedls, Rck/p54, and 4ET was confirmed by Western blotting or RT-PCR (Fig. S2, B and C), and their effect on PB integrity was confirmed by IF (Fig. S2 D). Representative cells are depicted, and the percentage of the transfected cells with S-foci in each treatment is indicated. Similar results were observed in three independent experiments. The bottom row shows enlarged views of the boxed regions. (D) U2OS cells were transfected with the indicated constructs, and the proportion of the transfected cells with foci is indicated. One representative experiment out of five is shown. (E) U2OS cells expressing the indicated constructs were treated with cycloheximide (CHX), emetine (EME), puromycin (PURO), or hippuristanol (HIP) during 4 h, and stained for DCP1a. The proportion of cells with foci relative to that of untreated cells for each construct and the proportion of cells with PBs identified by DCP1a are plotted. S-foci and PBs disassembled upon polysome stabilization by cycloheximide or emetine, whereas ΔSAM foci were fully resistant. Normalized values from 50 cells from a representative experiment out of three are shown. Error bars in E represents the standard deviation from triplicate coverslips. Bars: (A) 1 µm; (B–D) 10 µm.

mRNA-silencing foci, thus discarding the possibility of abnormal protein aggregation. Transient overexpression of translational repressors may induce SGs (Wilczynska et al., 2005; Thomas et al., 2011), and therefore we investigated the relationship of Smaug1-ECFP foci with SGs. We found that eIF3η, an obligate component of SGs, is not recruited to the Smaug1-ECFP foci (Fig. S2 A). However, as described previously (Baez and Boccaccio, 2005), the SG component TIA1/TIAR is present in a fraction of the larger Smaug1-ECFP foci (Fig. S2 A). This was restricted to the heterologous system, and TIA1/TIAR

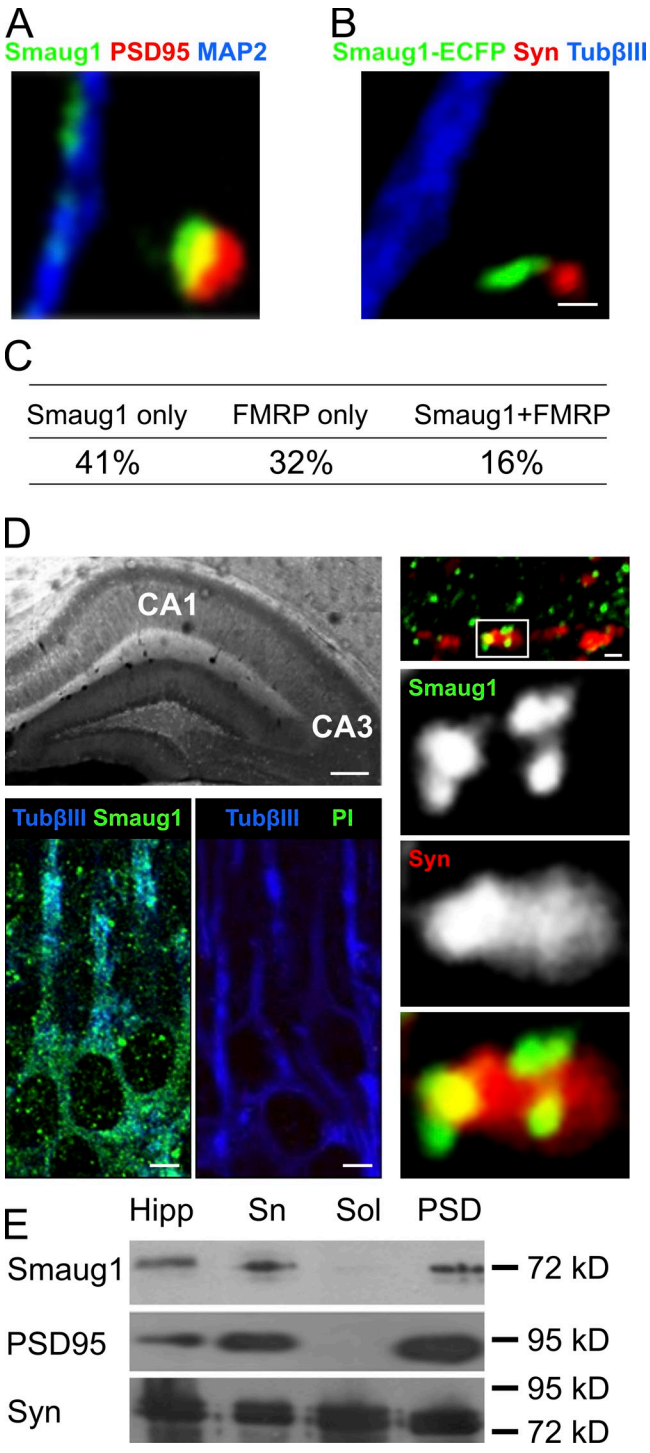

Figure 3. **Smaug1 foci at the postsynapse.** (A and B) Magnifications of isolated dendritic spines showing endogenous Smaug1 (A) or transfected Smaug1-ECFP (B), and the indicated markers. Endogenous or transfected Smaug1 form granules located at the postsynapse. (C) Smaug1 and FMRP were simultaneously stained in cultured neurons, and their presence in the synapses was evaluated. (D) Adult hippocampus slices were stained with the indicated antibodies. (D, top left) Tubulin βIII. (D, bottom left) A magnification of the CA1 region, including cell bodies and dendrites is shown. PI, rabbit preimmune serum. (D, right) A representative magnification of the CA3 region showing four S-foci associated with a synapse. Enlarged views of the boxed regions are shown below. (E) Synaptoneurosomes (Sn) were isolated from adult hippocampus (Hipp) by sucrose gradient centrifugation, then separated in a soluble extract (Sol) that was enriched in presynaptic components and that excluded PSD95, and a postsynaptic density-enriched fraction (PSD). Smaug1 is detected in the synaptoneurosomal and PSD fractions, and is absent from the soluble presynaptic fraction. Bars: (A and B) 1 µm; (D, left) 5 µm; (D, right) 1 µm.

was never observed in neuronal S-foci. A significant proportion of Smaug1-ECFP foci were in close contact, or virtually coincident with PBs visualized by DCP1a, Hedls, or RCK/p54 (Figs. 2 B and S2 A). Then, we investigated the effect of PB breakdown. We first provoked PB disassembly by knockdown of Hedls, Rck/p54, or 4ET, as described previously (Fenger-Grøn et al., 2005; Ferraiuolo et al., 2005; Thomas et al., 2009), and then transfected Smaug1-ECFP.

The knockdown was confirmed by Western blot analysis of Hedls and Rck/p54, and by RT-PCR for 4ET (Fig. S2, B and C). As expected, a strong reduction in the proportion of cells with PBs was observed upon treatment with the above siRNAs (Fig. S2 D). Then, we analyzed the presence of Smaug1-ECFP foci. Strikingly, we found that between 40 to 47% of the transfected cells formed S-foci in all cases, which indicates that the PB components Hedls, Rck/p54, or 4E are not required for S-foci assembly in cell lines (Fig. 2 C).

It has been suggested that the assembly of mRNA-silencing foci is a consequence of silencing (Eulalio et al., 2007; Thomas et al., 2011). We analyzed whether a Smaug1 truncate termed ΔSAM, which lacks the SAM domain that mediates RNA binding, was able to form foci (Fig. 2 D). As is the case for the full-length molecule, the ΔSAM foci were distinct from SGs (Fig. S2 A). We found that the SAM domain is dispensable for foci formation, and consistent with this observation, the isolated SAM domain did not form foci (Fig. 2 D). We speculate that the ΔSAM construct is not able to bind RNA, and thus we predict that ΔSAM foci will not respond to polysome stabilization, a distinctive feature of mRNA-silencing foci. As expected, we found that ΔSAM foci did not dissolve upon polysome stabilization by cycloheximide or emetine, whereas S-foci and PBs were significantly disassembled (Fig. 2 E), as described previously (Baez and Boccaccio, 2005). In spite of minor differences with neuronal S-foci, these observations in cell lines allowed us to conclude that S-foci formation is not the consequence of the binding to repressed mRNAs, and that neuron-specific factors are not required. In addition, S-foci formation is independent of PBs.

Synaptic Smaug1 silencing foci respond to NMDAR activation

Regulated translation is known to occur at postsynaptic sites (Steward et al., 1998; Huang et al., 2002; Antar et al., 2004; Shiina et al., 2005; Schratt et al., 2006). Thus, we analyzed the presence of Smaug1 silencing foci at the synapse surroundings. To identify synapses, we immunostained the presynaptic marker synapsin and the postsynaptic molecule PSD95 in cultured hippocampal neurons. We found that between 55 and 75% of synapses contain S-foci (Fig. 3 A). S-foci were detected in close contact with PSD95 clusters (Fig. 3 A), which suggests an association with the postsynaptic density, a scaffold structure that holds neurotransmitter receptors. In addition, we found that

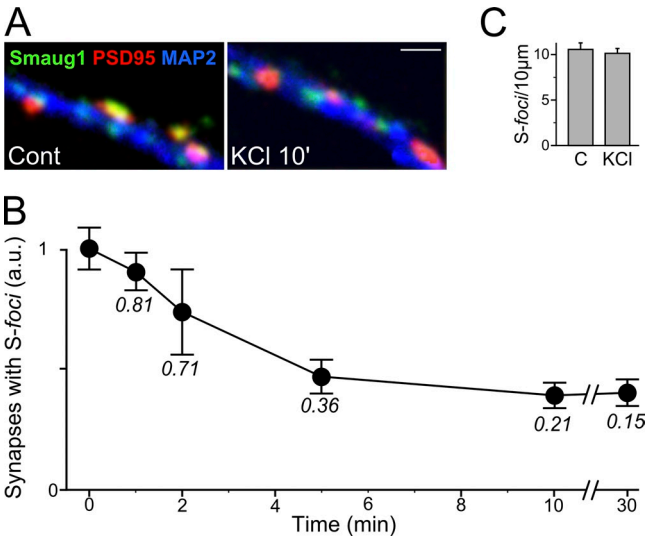

Figure 4. **S-foci located at postsynaptic sites respond to depolarization.** Hippocampal neurons were exposed to KCl as indicated in Materials and methods during the indicated time periods, and stained for the indicated proteins. (A) Representative dendrite fragments from control or depolarized neurons are shown. Synaptic Smaug1 signal is reduced in depolarized neurons. Bar, 1 µm. (B) The presence of S-foci in ~600 synapses from 40 random-selected dendritic fragments, and the S-foci size from 100 random selected S-foci was evaluated at the indicated time points. Normalized values and standard deviation from duplicates are shown (error bars). (C) The number of S-foci in dendrite shafts after a 10-min KCl pulse was evaluated in triplicate experiments. The number of synapses remained constant through the analyzed time points (not depicted).

transfected Smaug1-ECFP similarly formed granules present in the somatodendritic compartment and at postsynapses (Fig. 3 B). For comparison, we simultaneously investigated the presence of FMRP granules and found that most synapses contained FMRP and/or Smaug1, and that their presence was not mutually exclusive (Fig. 3 C).

We also analyzed the presence of Smaug1 granules in hippocampal slices (Fig. 3 D). Cell bodies and dendrites were strongly labeled by the anti-Smaug1 serum. In addition, Smaug1 granules frequently associated to synapsin clusters (Fig. 3 D). On average, 60% of synapsin patches contain one or two S-foci in their surroundings (Fig. 3 D, insets). Finally, we found that Smaug1 is present in hippocampal synaptosomes isolated by sucrose gradient centrifugation (Fig. 3 E). Moreover, Smaug1 copurified with PSD95 in postsynaptic densities isolated from synaptosomes by extraction with Triton X-100 at pH 8.0 (Phillips et al., 2001). Smaug1 is absent from the soluble fraction obtained by this procedure, which is enriched in presynaptic components and excludes postsynaptic molecules (Fig. 3 E; Phillips et al., 2001).

Translation at the postsynapse is finely regulated by synaptic stimulation, and we hypothesized that Smaug1-mediated repression is modulated by synaptic activity. We reasoned that if mRNA silencing by Smaug1 is released upon synaptic stimulation, the number and/or size of the S-foci will decrease. Conversely, the presence of S-foci is expected to increase if synaptic stimulation enhances repression by Smaug1. Then, we exposed neurons to a short depolarizing stimulus by increasing potassium concentration to 40 mM. We found that the number of synapses containing S-foci was significantly reduced upon stimulation (Fig. 4 A). The response was rapid; it was detected 1 min after depolarization, and 5 min after the stimulus the proportion of synapses with S-foci was reduced to 50% relative to basal levels. In addition, the size of the remaining S-foci was significantly reduced. A prolonged treatment of 30 min did not further increase the response (Fig. 4 B). S-foci dissolution was reversible, and 16 h later the presence of S-foci at synapses was fully recovered (unpublished data). Remarkably, the effect was observed in the S-foci associated with the synapses, identified by PSD95 or synapsin staining, whereas the S-foci located in the dendritic shaft were not significantly altered, which suggests that the dissolution of the S-foci involves a local response (Fig. 4, B and C).

We then investigated which synaptic receptors mediate S-foci dissolution. Most stimulatory hippocampal synapses respond to glutamate, whereas inhibitory synapses in these cells respond to γ-amino butyric acid (GABA). Next, we applied a short depolarizing stimulus in the presence of kynurenic acid, a blocker of the ionotropic glutamate receptors that respond to α-amino-3-hydroxy-5-methyl-4-isoxazolepropionic acid (AMPA) or to NMDA. The effect of picrotoxin, a GABA-A receptor inhibitor, was also analyzed. We found that glutamate receptor blockage completely abrogated the dissolution of S-foci triggered by depolarization, whereas GABA-A receptor inhibition did not affect the response (Fig. 5 A).

Next, we investigated which glutamate receptor is involved. We used the NMDA antagonist 2-amino-5-phosphonopentanoate (APV) and the AMPA antagonist 6-cyano-7-nitroquinoxaline-2,3-dione (CNQX). We found that NMDAR inhibition completely abrogated the response to depolarization, whereas AMPA receptor (AMPAR) inhibition had no effect on the dissolution of the S-foci triggered by KCl-mediated depolarization (Fig. 5 B). For comparison, we simultaneously analyzed the response of the FMRP granules. We found that FMRP granules responded to AMPAR activity, in agreement with a previous study (Antar et al., 2004). In addition, we found that in contrast to the S-foci, FMRP granules were not affected by NMDAR activity (Fig. 5 C).

To further assess the role of NMDAR in S-foci dynamics, we exposed hippocampal neurons to a short pulse of NMDA. Before stimulation, hippocampal cells were treated with tetrodotoxin (TTX), which blocks the opening of the voltage-gated Na^+ channel, thus leading to a depressed state. This treatment did not affect the S-foci significantly. TTX-treated neurons were stimulated over 5 min with 30 µM NMDA and allowed to recover. The number and size of the S-foci at synapses were measured at several time points after the stimulus. In agreement with the above results, we found that the S-foci dissolved upon NMDAR activation. The effect was immediate and reversible. 5 min after NMDA exposure, the number of synapses containing S-foci was reduced to <50% relative to basal levels (Fig. 5 D), and the remaining foci were significantly smaller (0.52 μm^2 in resting conditions vs. 0.37 μm^2 immediately after the NMDA pulse). The effect lasted for 60 min after release of the stimulus, and cells started to recover within 6 h afterward (Fig. 5 D).

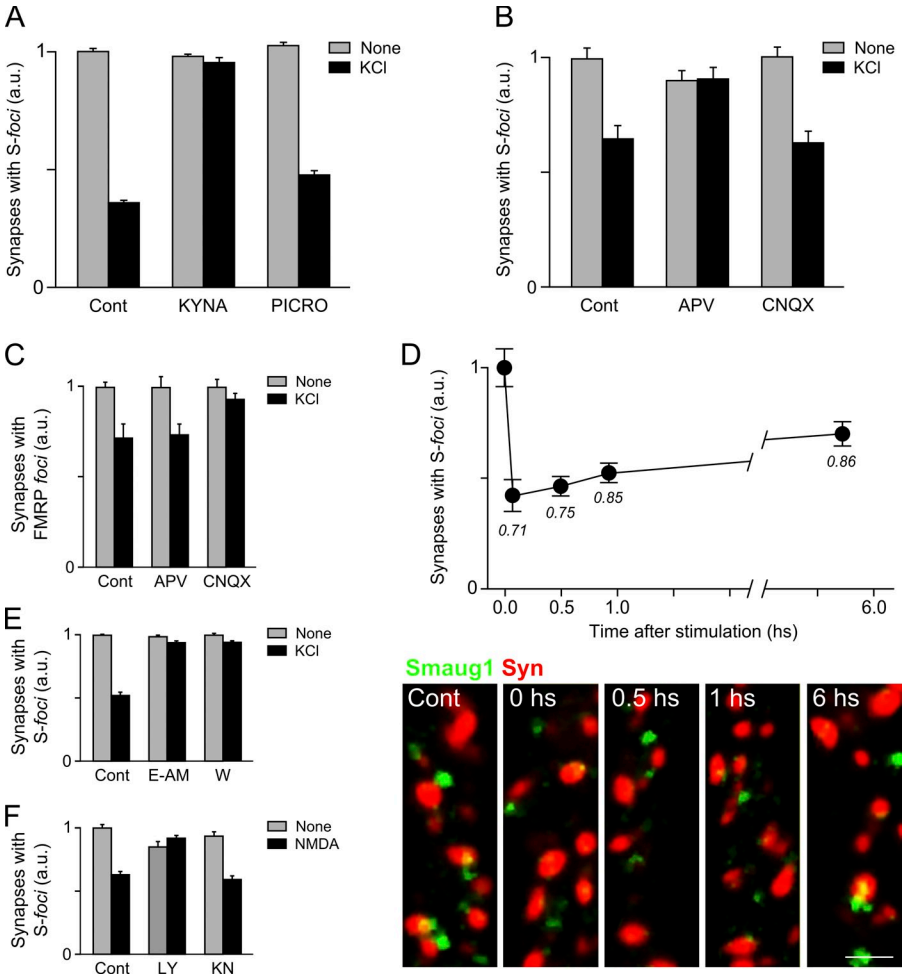

Figure 5. **S-foci respond to NMDAR activation.** (A–C) Hippocampal neurons were exposed to KCl during 10 min in the presence or absence of the indicated drugs, and the number of synapses with associated Smaug1 (A and B) or FMRP granules (C) was evaluated. KYNA, kynurenic acid; PICRO, picrotoxin. (D) Neurons were pulsed with NMDA as indicated in Materials and methods and allowed to recover, and the presence of S-foci at the synapses was analyzed. S-foci size normalized to control values at each time point is indicated. Similar results were observed in three independent experiments including different time points. (D, bottom) Representative IF images corresponding to the experiments depicted. Bar, 1 µm. (E and F) Neurons were exposed to KCl or NMDA in the presence of the indicated drugs, and the presence of S-foci associated to synapses was evaluated as in Fig. 4 B. E-AM, EGTA-AM; W, wortmannin; KN, KN93; LY, LY294002. Approximately 100 dendritic fragments from 20 neurons were analyzed for each data point. Error bars indicate standard deviation from triplicate coverslips in a representative experiment.

Next, we investigated whether calcium influx is involved in the response. We treated the neurons with the intracellular calcium chelator EGTA-AM shortly before and also during the depolarization stimulus. We found that intracellular Ca depletion abrogates S-foci dissolution, which indicates that calcium influx mediates the response (Fig. 5 E). Phosphoinositide 3-kinase (PI3K) and CaMKII are relevant kinases that are locally stimulated by calcium influx upon NMDA activation. To investigate the participation of these signaling pathways, we used pharmacological inhibitors: wortmannin or LY294002 against PI3K, and KN-93 against CaMKII. We found that PI3K inhibition blocked S-foci dissolution triggered either by KCl-mediated depolarization (Fig. 5 E) or by NMDAR activation (Fig. 5 F). Inactivation of CaMKII had no effect (Fig. 5 F). Whether Smaug1 is directly affected by PI3K remains to be investigated.

Smaug foci disassembly upon synaptic stimulation requires polysome assembly

We speculated that S-foci dissolution upon synaptic stimulation is linked to mRNA release and translation activation. Thus, we analyzed the effect of translational blockers that enhance or impair polysome stability. We found that cycloheximide or emetine, which provoke polysome stalling, did not affect the dissolution of the S-foci triggered by either KCl or NMDA (Fig. 6, A and B; and not depicted). In all cases, the number of synapses containing S-foci and the foci size were significantly reduced. In striking contrast, puromycin or hippuristanol, which impair polysome assembly, completely abrogated the response triggered by depolarization or by direct NMDAR activation (Fig. 6, A and B).

These results are compatible with the notion that S-foci dissolution upon NMDAR activation allows the release of silenced mRNAs and their recruitment to polysomes. When polysome assembly is impaired, mRNAs would return to the S-foci, counteracting the dissolution triggered by synaptic stimulation.

We wondered whether S-foci plasticity involves Smaug1 degradation during dissolution and de novo synthesis to allow reassembly. Against this possibility, we found that S-foci dissolution upon depolarization was not affected by the presence of the proteasome inhibitor MG132 (unpublished data). In addition, we followed S-foci dissolution and reassembly in the absence of protein synthesis, and found that the synthesis of new Smaug1 molecules is not required during aggregation (Fig. 6 C). As in Fig. 6 (A and B), polysome-stabilizing drugs did not impair S-foci dissolution by NMDAR stimulation, and as expected (Fig. 5 D), S-foci remained disassembled for up to 1 h afterward (Fig. 6 C). S-foci recovery was enhanced in the presence of the translational inhibitor puromycin, which suggests that Smaug1 molecules cycle between aggregated and disaggregated states to regulate the availability of specific transcripts.

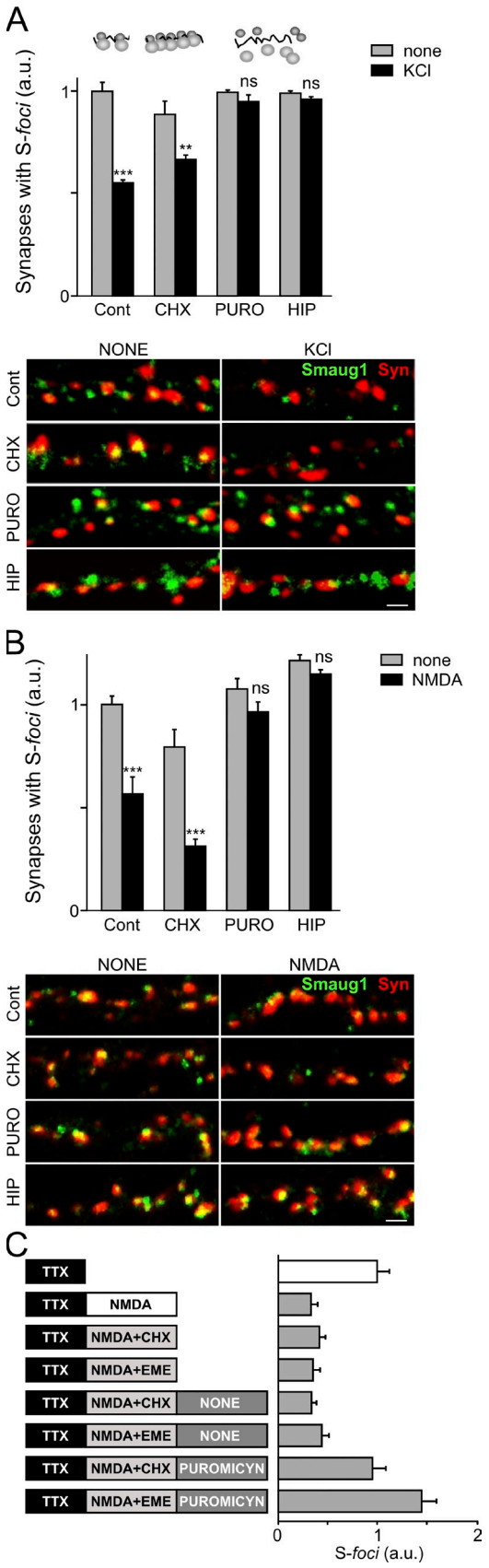

Figure 6. **S-foci dissolution upon synaptic stimulation requires polysome assembly.** (A–C) Hippocampal neurons were exposed to KCl or NMDA as indicated in Materials and methods, in the presence or absence of the indicated translation inhibitors. CHX, cycloheximide; PURO, puromycin; Hip, hippuristanol. (A and B) The proportion of synapses containing S-foci relative to basal levels from three independent experiments is plotted, and IF images of representative dendritic fragments for the indicated treatments are depicted. Bars, 1 µm. (C) TTX-silenced hippocampal cells were stimulated with NMDA in the presence or absence of cycloheximide or emetine (EME), which stall polysomes, and allowed to recover during 60 min, in the presence or absence of puromycin, which disrupts polysomes. S-foci were analyzed as in Figs. 4 and 5. The continuous inhibition of protein synthesis does not affect S-foci reassembly. Similar results were obtained in a duplicate experiment. Approximately 50 dendritic fragments (total length, 750 µm) from 20 neurons were analyzed for each data point. Error bars indicate standard deviation.

NMDA induces the dissociation of Smaug1 from CaMKIIα mRNA granules

CaMKIIα mRNA is known to be locally translated upon NMDA stimulation (Huang et al., 2002; Banerjee et al., 2009), and thus we sought to investigate whether the S-foci are involved in the regulation of this messenger. First, we analyzed whether Smaug1 and CaMKIIα mRNA colocalize. We performed FISH analysis and found that, as reported before, this transcript is present in granules in the soma and dendrites. Simultaneous staining of Smaug1 revealed that a significant proportion of CaMKIIα mRNA granules are associated with S-foci (Fig. 7 A). Both in the dendritic shaft and at the synapse surroundings, 45% of CaMKIIα mRNA granules associated with S-foci at a distance <150 nm (averaged from three independent stainings), which is compatible with a intermolecular interaction, as described for other RBPs and their target mRNAs (Giorgi et al., 2007).

Next, we investigated whether this association is affected by NMDAR stimulation. After a 5-min NMDA pulse, neurons were stained for CaMKIIα mRNA, Smaug1, and synapsin. As before (Figs. 5 D and 6 B), NMDA exposure provoked the dissolution of the synaptic S-foci, which were reduced from 50 ± 3% to 32 ± 2% (Fig. 7 B). In addition, we found that the presence of CaMKIIα mRNA granules at the synapse was enhanced by NMDAR stimulation, thus paralleling the recruitment of this messenger upon stimulation of metabotropic receptors (Kao et al., 2010). The proportion of synapses with CaMKIIα mRNA granules increased from 33 ± 3% to 43 ± 3% (Fig. 7 B). Importantly, in spite of this increase on the number of synapses with CaMKIIα mRNA, the number of synapses where CaMKIIα mRNA colocalized with S-foci was reduced to half the normal values. In resting conditions, 16 ± 2% of the synapses contain CaMKIIα mRNA granules that colocalize with S-foci, and this value dropped to 8 ± 1% upon the NMDA pulse (Fig. 7 B). Overall, colocalization at the synapse was reduced from 50 ± 3% to 18 ± 3% upon NMDA exposure (Fig. 7 B). The effect was not restricted to the synapses, and in the dendritic shaft the colocalization between CaMKIIα mRNA granules and S-foci dropped from 45 ± 5% to 30 ± 2%. Whether CaMKIIα mRNA molecules free of Smaug1 represent translating mRNA molecules remains to be investigated. Supporting this possibility, it was recently shown that CaMKIIα mRNA in dendrites is mostly found as a single molecule, and thus, we speculate that either repressed or polysome-engaged CaMKIIα mRNA may render similar discrete stainings. Finally, as expected, we found that CaMKII levels increased

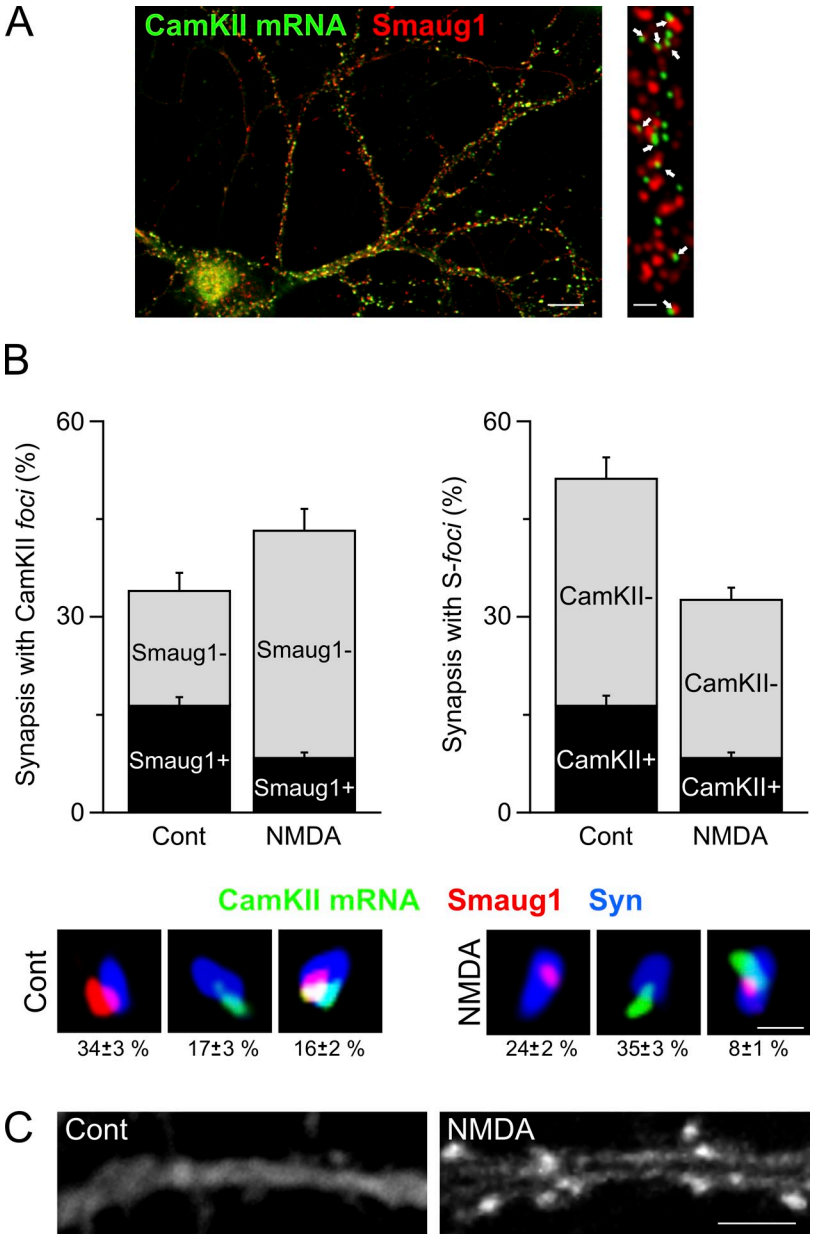

Figure 7. **CaMKIIα mRNA associates to S-foci in an activity-dependent manner.** (A) CaMKIIα mRNA and Smaug1 were simultaneously detected by FISH and IF, respectively. Between 40 and 60% of CaMKIIα mRNA granules colocalize or are in close contact with S-foci. A representative dendrite is shown. (B) Neurons were stimulated with NMDA during 5 min and stained for CaMKIIα mRNA, Smaug1, and synapsin. The number of CaMKIIα mRNA granules at the synapse, associated to S-foci (S+) or not (S−), and the number of synaptic S-foci, associated to CaMKIIα granules or not, are plotted. Approximately 300 synapses from 20 random selected neurons were analyzed in each case. Error bars indicate standard deviation. (B, bottom) Representative immunofluorescent images of synaptic S-foci and CaMKIIα mRNA granules either colocalizing or not colocalizing for each condition. The percentage relative to the total number of synapses and standard error is indicated in each case. (C) Neurons were stimulated with NMDA during 5 min and immunostained for CaMKIIα 30 min after the pulse. Representative dendritic fragments showing an increase of CaMKII signal at the dendritic spine are depicted. Bars: (A, left) 10 µm; (A, right) 1 µm; (B) 1 µm; (C) 2 µm.

locally after NMDA stimulation, as judged by IF analysis with a specific antibody (Fig. 7 C).

Then, we investigated whether S-foci dissolution by NMDA correlates with a global stimulation of local translation. We used the recently developed fluorescent noncanonical amino acid tagging (FUNCAT) strategy, which was successfully used to demonstrate changes in local translation in dendrites upon exposure to brain-derived neurotrophic factor (BDNF; Dieterich et al., 2010). In brief, neurons were pulsed with the methionine surrogate azidohomoalanine (AHA) to evaluate basal synthesis, then exposed to NMDA and incubated for variable time periods with a second methionine substitute, homopropargylglycine (HPG; see Materials and methods). Then, incorporated AHA and HPG were covalently tagged with specific fluorescent molecules, and signal intensities were determined by confocal microscopy. First, we assessed whether incorporation of these noncanonical amino acids was blocked by translation inhibitors. We found that cycloheximide completely abrogates the signal in both cell soma and dendrites of both AHA and HPG, which were incorporated linearly during at least 1 h (Fig. 8, A and B; and not depicted). Then we performed a sequential metabolic labeling to asses the effect of NMDA in local translation at dendrites. We found that a short treatment with NMDA significantly blocked the incorporation of labeled amino acids (Fig. 8, B and C). The effect was immediate, and three independent experiments showed a reduction of protein synthesis to 42–54% relative to nonstimulated neurons during the first 30 min (Fig. 8, B and C; and not depicted). Local translation slowly recovered, but it was still significantly lower 60 min after the stimulus. All these observations suggest that local NMDAR activation provokes a global translational silencing, and at the same time allows the translation of CaMKIIα mRNA and other unknown mRNAs by triggering S-foci dissolution.

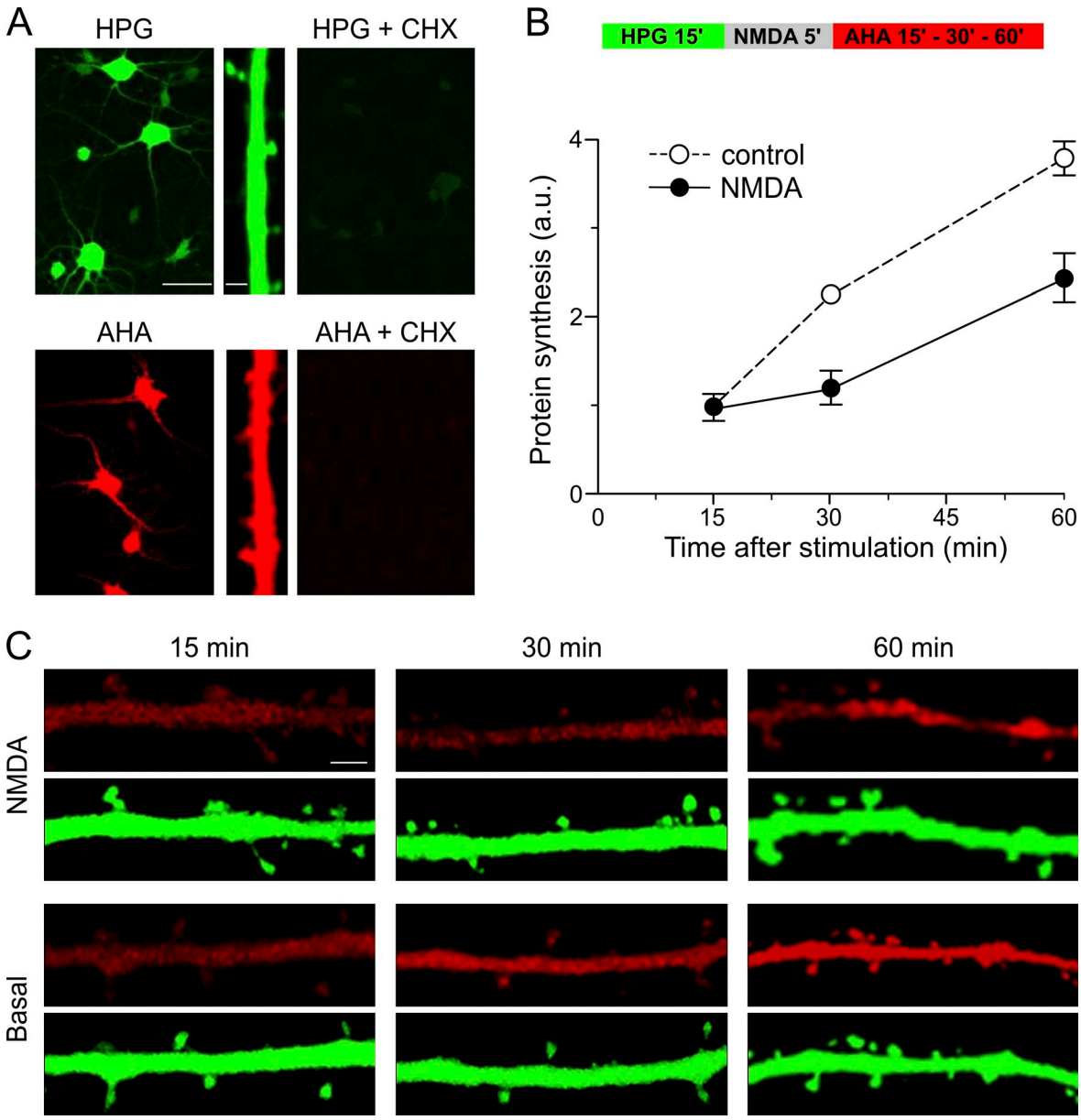

Figure 8. **NMDAR activation inhibits global translation at the dendrite.** The FUNCAT strategy was used as indicated in Materials and methods. (A) Cultured neurons were pulsed with HPG or AHA in the presence or absence of cycloheximide (CHX), and the incorporated modified amino acids were covalently coupled to Alexa Fluor 488 or 595. Translation inhibition completely abrogated the signal. Insets show representative dendrite fragments. Bars: (left) 20 µm; (right) 1 µm. (B) HPG and AHA were used sequentially to evaluate the protein synthesis rate before and after the stimulus, respectively. HPG and AHA signal intensities were measured in ~40 dendrite fragments (total length, 800 µm) for each time point. AHA incorporation at different times after stimulation relative to basal HPG incorporation is plotted. One representative experiment out of four is depicted; error bars indicate the standard deviation from triplicate coverslips. (C) Representative dendrite fragments showing the NMDA inhibitory effect on protein synthesis in dendrite shafts and spines. Bar, 1 µm.

Smaug1 affects synapse formation

Translational regulation at the synapse is important for synapse remodeling and stabilization. Having demonstrated that Smaug1 forms mRNA-silencing foci that respond to synaptic stimulation, apparently regulating the key transcript encoding CaMKIIα, among others, we then investigated whether Smaug1 affects synapse formation or function. First, we investigated the expression of this protein during neuron development in vitro by Western blot analysis of Smaug1 and selected synapse components (Fig. 9 A). We found that Smaug1 expression was negligible during the first week, and that this molecule began to accumulate simultaneously with synapsin and PSD95 after the eighth day in culture (Fig. 9 A). In contrast, as expected, we found that FMRP and Staufen1 were constitutively expressed (unpublished data). Thus, Smaug1 expression coincides with synaptogenesis in cultured hippocampal neurons.

To investigate the role of Smaug1 in synaptogenesis, we treated hippocampal cells at the sixth day in culture with a pool of siRNAs against Smaug1 (siSmaug1). RT-PCR analysis performed after 15 d in culture indicated that Smaug1 mRNA levels were reduced to 10% relative to control levels. Efficient depletion of the protein was confirmed by Western blotting and

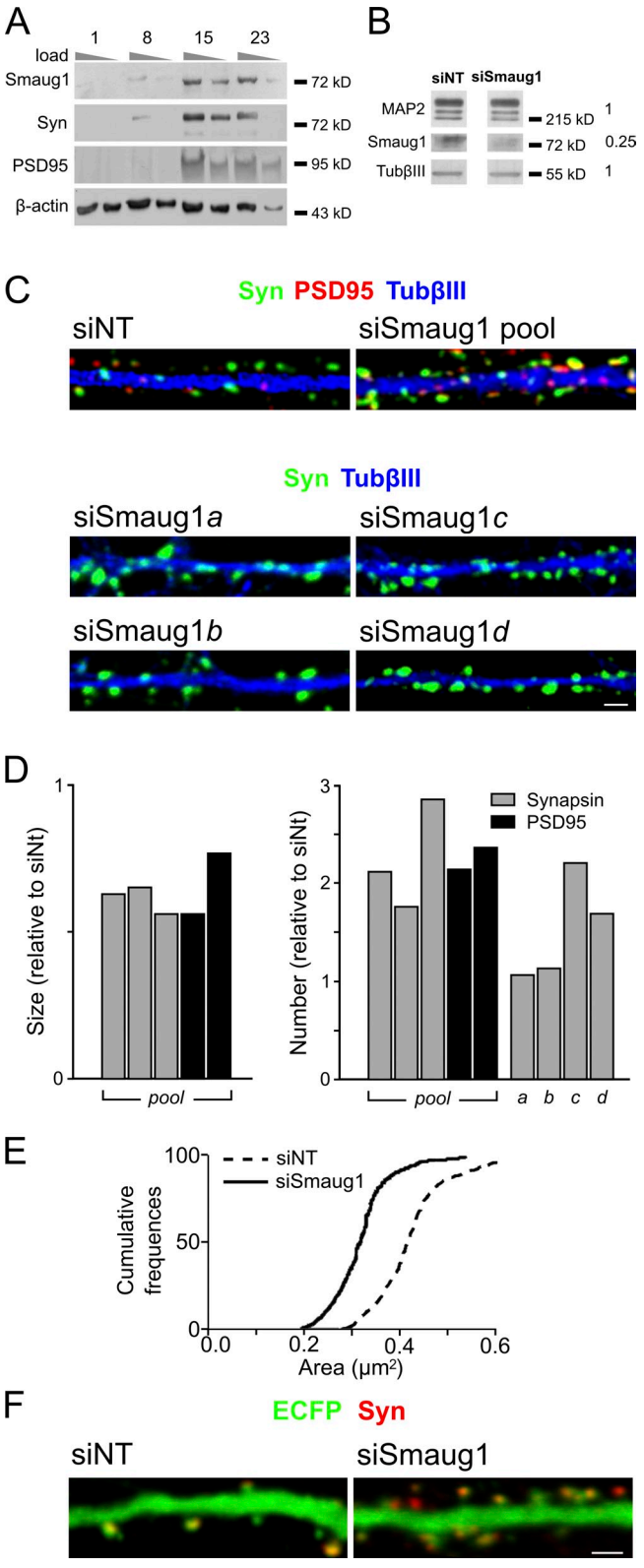

Figure 9. **Smaug1 knockdown affects synapse size and number.** (A) Western blot of postnuclear protein extracts (10 or 5 μg) from cultured hippocampal neurons at 1, 8, 15, or 23 d in vitro with the indicated antibodies. (B–F) Neurons were treated with the indicated siRNAs as described in Materials and methods. (B) Smaug1, Map2, and tubulin βIII levels were evaluated by Western blotting. Signal intensity relative to that of β-actin is indicated. An siRNA against Smaug 2 had no effect on Smaug1 levels (not depicted). (C) Representative dendrite fragments stained with the indicated synapse or cytoskeleton markers are shown. (D and E) The size and number of synaptic puncta identified by simultaneous or independent staining of PSD95 and synapsin was measure as indicated in Materials and methods. (D) Summary of the normalized synapse size and number relative to that of siNT-treated neurons in three independent experiments with the siSmaug1 pool, and in a representative experiment comparing the four different siRNA. (E) Synapse size distribution in a representative experiment with the siSmaug1 pool. Random selected dendritic fragments from 10 neurons (total length, 5,000 μm) were analyzed in each case. (F) Neurons were transfected with ECFP and treated with the indicated siRNAs as indicated in Materials and methods. Representative dendrite fragments stained for ECFP and synapsin are shown. Dendritic spines were more numerous upon Smaug1 depletion. Bars, 2 μm.

IF analysis (Figs. 9 B and S1 C). Strikingly, an alteration in synapse puncta was observed in siSmaug1-treated cells. We found that both PSD95 and synapsin clusters were smaller and more numerous than in control or siNT-treated cells (Fig. 9 C and not depicted). A quantitation of these parameters in five independent experiments indicated that Smaug1 knockdown reduced synapse size to 65% of normal values, and provoked a duplication or triplication of their number (Fig. 9, D and E). To rule out off-target effects, the four RNAi sequences present in the siSmaug1 pool were analyzed separately. We found that two of them provoked an alteration in synapse number and size comparable to the effect of the pool (Fig. 9, C and D); all this indicates that the effect is specific to Smaug1 knockdown.

PSD95-containing synapses in hippocampal cells are mostly excitatory, and are located in dendritic spines. To visualize dendritic spines, neurons were transfected with ECFP and stained for PSD95 (Fig. 9 F). As expected, PSD95 clusters were located at the tip of dendritic spines. Remarkably, dendritic spines were longer and thinner in siSmaug1-treated cells, thus resembling an immature morphology.

Finally, we wondered whether this morphological alteration impaired synapse excitability. To investigate this, we exposed hippocampal neurons to a repeated depolarizing stimuli, which simulates a long-term potentiation (LTP)-like response (Wu et al., 2001), and stained the cells for the early activity-related marker Arc/Arg3.1 (Steward et al., 1998; Steward and Worley, 2001). As expected, we found that Arc/Arg3.1 was rapidly induced in control or siNT-treated neurons (Fig. 10, A and B). In these cells, the Arc/Arg3.1 signal intensity doubled at 60 min after stimulation. In striking contrast, Arc/Arg3.1 expression was virtually not induced in siSmaug1-treated neurons (Fig. 10 B). Altogether these observations indicate that Smaug1 knockdown alters synapse size and number, and concomitantly provokes a defective synaptic response.

Discussion

In this paper, we describe for the first time the existence of a novel kind of mRNA-silencing foci specific to neurons. These silencing foci, which we named S-foci, contain mammalian Smaug1/Samd4A, an RNA-binding protein that belongs to a novel family of posttranscriptional regulators. S-foci are distinct from PBs and SGs, and from other neuronal RNA granules hitherto described (for reviews see Kiebler and Bassell, 2006; Anderson and Kedersha, 2009; Buchan and Parker, 2009;

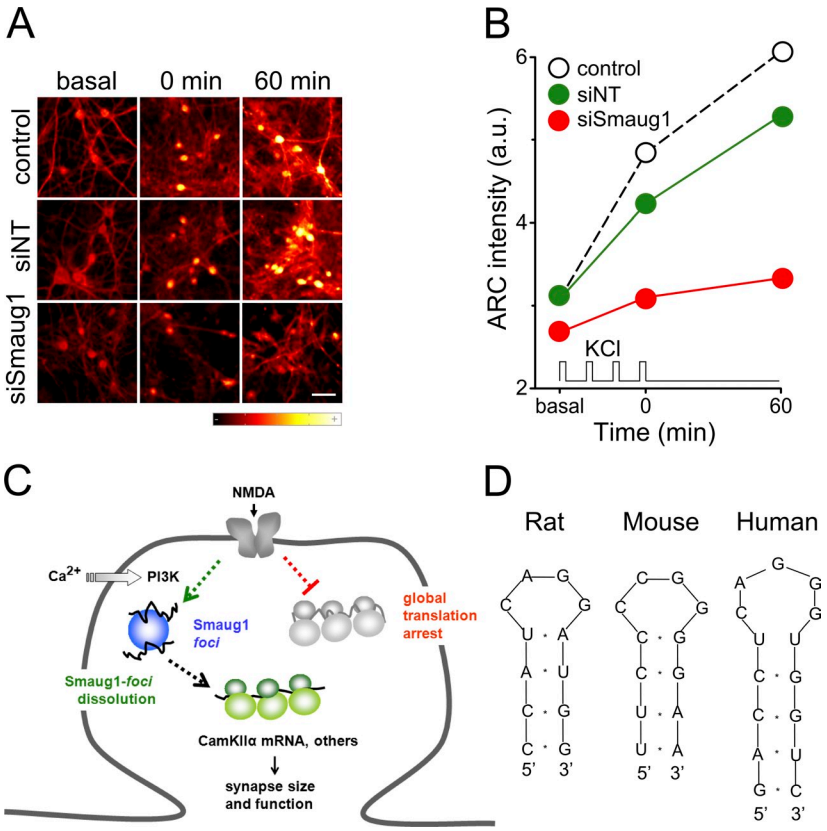

Figure 10. **Smaug1 knockdown affects neuron excitability.** Neurons were treated with the indicated siRNA and exposed to a repeated depolarizing stimulus. (A) Arc/Arg3.1 was detected by IF at the indicated times and shown in glow scale. Bar, 20 µm. (B) Integrated intensity in the cell bodies from 100 neurons from duplicate coverslips was quantified in 20× micrographs. A duplicate experiment with similar results was performed. (C) Hypothetical model for a role of Smaug1 in local translation at the synapse and its regulation by NMDA. CaMKIIα mRNA and other repressed transcripts would be associated with the S-foci, likely as single molecules (see Discussion; Mikl et al., 2011). Upon NMDAR stimulation, the S-foci dissolve, likely facilitating the translation of selected mRNA. Simultaneously, local translation is globally repressed. Local translation of CaMKIIα is known to mediate synapse strength, and additional unknown transcripts regulated by Smaug1 may also contribute. (D) Putative SREs are present in the 3′ UTR of CaMKIIα mRNAs from distinct species. In addition, conserved putative SREs are present at the coding region (not depicted).

Martin and Ephrussi, 2009; Thomas et al., 2011). Like PBs, the S-foci behave as mRNA-silencing foci, as they are able to release transcripts allowing their incorporation to polysomes. Relevantly, S-foci dynamics depend greatly on neuron activity, and our observations suggest that the CaMKII mRNA, and likely other unknown transcripts, cycle between S-foci and polysomes in an activity-dependent manner, thus paralleling the cycling of specific mRNAs between PBs and polysomes in other cellular contexts. We speculate that similar foci exist in *Drosophila* peripheral neurons, where dSmaug regulates specific mRNAs (Brechbiel and Gavis, 2008). Supporting this assumption, *Drosophila* Smaug is found in foci in fly embryos and forms granules when expressed in cell lines (Baez and Boccaccio, 2005; Zaessinger et al., 2006; Rouget et al., 2010).

The molecular mechanism for mRNA repression by mammalian Smaug1 is unknown. *Drosophila* Smaug acts by two pathways: it represses translation by blocking initiation at the level of 4E–4G interaction and by capturing target transcripts in repressed RNP complexes (Jeske et al., 2011). In addition, *Drosophila* Smaug initiates mRNA decay by triggering deadenylation (Nelson, et al., 2004; Zaessinger, et al., 2006; Tadros, et al., 2007; Rendl et al., 2008; Rouget, et al., 2010). Paralleling the functions of the *Drosophila* molecule, mammalian Smaug1 may block initiation, may mediate deadenylation, which is frequent in neuronal mRNAs (Du and Richter, 2005), or may govern the formation of masking RNPs where mRNAs are sequestered from translation factors. All these mechanisms are compatible with the formation of Smaug1 mRNA-silencing foci. Whether Smaug1 aggregation in discrete structures is required for efficient mRNA repression is unknown. Several proteins involved in mRNA silencing have distinct oligomerization domains (Franks and Lykke-Andersen, 2008; Salazar et al., 2010; Thomas et al., 2011), and how aggregation contributes to mRNA repression is a matter of debate. Nevertheless, our finding that S-foci formation does not require binding to RNA indicates that aggregation is not a consequence of mRNA silencing, and supports the hypothesis that the formation of oligomeric structures is important for Smaug1 function. Transcripts located at the synapses are transported relatively long distances from the cell body, and this transport is performed in granules (Knowles et al., 1996; Köhrmann et al., 1999; Steward and Worley, 2001; Kanai et al., 2004; Falley et al., 2009; Martin and Ephrussi, 2009). Thus, besides putatively enhancing translational repression by physical sequestration of mRNAs, the self-aggregation of a translational regulator may contribute to the assembly of transport-competent complexes carrying repressed mRNAs. Conversely, dissolution of S-foci upon synaptic stimulation may contribute to restrict the movement of transcripts that are required at the synapse. The molecular mechanism underlying S-foci aggregation is unknown, and is likely to involve oligomerization domains and motor molecules, which govern the assembly of mRNA-silencing foci in general (Franks and Lykke-Andersen, 2008; Loschi et al., 2009; Salazar et al., 2010).

We found that mammalian S-foci associate to synapses and selectively respond to NMDAR activation, dissolving and facilitating the translational activation of CaMKIIα mRNA and a plethora of unknown transcripts. The response is immediate and transient, and involves calcium influx and PI3K signaling (see the hypothetical model in Fig. 10 C). Whether Smaug1 oligomerization is directly controlled by this signaling

pathway remains to be investigated. We found that AMPAR or GABAR activity do not affect S-foci dynamics. In contrast, FMRP granules respond to AMPAR stimulation (this paper and Antar et al., 2004), which indicates that distinct neuronal granules specifically respond to distinct stimuli. Further supporting a remarkable specificity of the response, we found that while Smaug1-mediated repression is released, NMDAR stimulation globally inhibits local protein synthesis, in agreement with previous studies (Leski and Steward, 1996; Marin et al., 1997; Scheetz et al., 2000; Sutton et al., 2004, 2006, 2007; Schuman et al., 2006).

The messenger encoding CaMKIIα is activated by NMDAR stimulation via several mechanisms, including cytoplasmic polyadenylation and relief from microRNA silencing (Scheetz et al., 2000; Steward and Worley, 2001; Huang et al., 2002; Ashraf et al., 2006; Bramham et al., 2008), all compatible with the Smaug1-mediated repression suggested here. Human Smaug1 recognizes the SRE motifs from the *Drosophila* nanos mRNA (Baez and Boccaccio, 2005), and thus we speculate that the transcripts regulated by mammalian Smaug1 will contain related motifs. A putative SRE is present in the 3′ untranslated region (UTR) of the human, rat, and mouse CaMKIIα (Fig. 10 D). The relevance of these elements in the regulation of CaMKIIα mRNA by Smaug1 remains to be investigated. It is well established that CaMKIIα affects spine size and synaptic function (Pi et al., 2010), and thus, we speculate that dysregulation of this messenger contributes to the serious synaptic defect provoked by Smaug1 depletion.

Smaug1 is expressed late during neuronal differentiation, coincident with the expression of key synaptic components and with the appearance of visible synaptic contacts. Several mRNAs relevant to synapse function start to accumulate at this developmental time (Paradis et al., 2007), and thus Smaug1 may have a role in the local control of these new mRNAs. In addition to its contribution to the regulation of local translation by synaptic stimulation, we speculate that Smaug1 helps the profound remodeling of the transcriptome that occurs during synaptogenesis (Paradis et al., 2007). We speculate that, paralleling the role of *Drosophila* Smaug during the maternal-to-zygotic transition, during which fly Smaug down-regulates hundreds of maternal mRNAs (Tadros et al., 2007; Benoit et al., 2009), mammalian Smaug1 may be involved in a massive silencing of early mRNAs that are not required after synaptogenesis. These putative Smaug1 mRNA targets remain to be identified. SREs may have loops up to seven nucleotides long, and the secondary structure that surrounds the motifs may affect their accessibility (Aviv et al., 2003, 2006; Green et al., 2003; Johnson and Donaldson, 2006; Oberstrass et al., 2006; Foat and Stormo, 2009; Li et al., 2010; Ravindranathan et al., 2010). Thus, the identification of mammalian Smaug1 targets will require intense investigation.

Materials and methods

Neuron culture, cell lines, and transfection

U2OS and HeLa cells were from the American Tissue Culture Collection and grown and maintained as indicated. Hippocampal cultures were prepared as described previously (Banker and Goslin, 1998). In brief, hippocampi were dissected from Sprague Dawley rats at embryonic day 18 and digested with trypsin. Cells were seeded on poly-D-lysine (Sigma-Aldrich)-coated glass coverslips. Cultures were maintained in Neurobasal medium (NB; Invitrogen) supplemented with B27 (Invitrogen) and glutamine (complete NB; Invitrogen) at 5% CO_2. Cell lines were transfected with either Lipofectamine 2000 Transfection Reagent (Invitrogen) or Jet Prime (Polyplus Transfection) according to manufacturer's instructions. Neurons were transfected one day after plating using Lipofectamine 2000 Transfection Reagent (Invitrogen) during 4 h, and analyzed at day 15. The following constructs were used: (a) A full-length Smaug1 fused to either EGFP or V5 (Baez and Boccaccio, 2005). (b) ECFP-ΔSAM, including two fragments of hSmaug1: amino acids 1–317 fused to amino acids 376–717 and tagged with ECFP in the N terminus. An hSmaug1 fragment spanning amino acids 1–376 was PCR-amplified from the pCDNA6–V5–hSmaug1 described previously (Baez and Boccaccio, 2005) using 5′-TAATACGACTCACTATAGGG-3′ and 5′-AAGGCGAGCCTCGAGGGTG-3′ as primers, digested with HindIII and XhoI, and inserted between the HindIII and SalI sites of pECFP-C3 (Takara Bio Inc.). A second amplification was performed with 5′-GCGAGCCTCGGGTGTGTTACGAGC-3′ and 5′-CATGGTCCTGCTGGAGTTCGTG-3′ as primers. The hSmaug1 N-terminus hSmaug1 including amino acids 376–717 was amplified using 5′-GCTCGTAACACACCCGAGGCTCGC-3′ and 5′-CGTCGCCGTCCAGCTCGACCAG-3′ as primers. The last two PCR products contained a 12-bp overlapping region, and were fused by splicing with overlapping extension PCR (SOE-PCR), using the primers 5′-CGTCGCCGTCCAGCTCGACCAG-3′ and 5′-CATGGTCCTGCTGGAGTTCGTG-3′. This PCR product was digested with HindIII and BamHI and inserted between the HindIII and BamHI site of the pECFP-N1 plasmid (Takara Bio Inc.). (c) ECFP-SAM: The region encoding the RBD was PCR-amplified from a hSmaug1-ECFP construction (Baez and Boccaccio, 2005) using the primers 5′-CCGCTGCTCGGAATTCATTCCA-3′ and 5′-AAGGCGAGCCTCGAGGGTG-3′, digested with EcoRI and XhoI, and inserted between the EcoRI and SalI sites of the pECFP-C1 plasmid (Takara Bio Inc.).

siRNA treatment

U2OS cells were treated with a nontargeting siRNA (siNT) 5′-UAGCGACUAAACACAUCAA-3′; an siRNA anti-Hedls (siHedls, catalog no. 004397; Thermo Fisher Scientific); anti-Rck/p54 (siRck/p54, catalog no. 0143295); or an siRNA against 4ET (5′-GAACAAGAUUAUCGACCUA-3′; Ferraiuolo et al., 2005) used at 50 nM, and transfected 72 h afterward with the indicated plasmids. Jet Prime was used for both steps. Hippocampal neurons were allowed to grow for 6 d in vitro, incubated with 100 nM siRNA (Thermo Fisher Scientific) complexed with Lipofectamine 2000 Transfection Reagent (Invitrogen) for 4 h, and analyzed at 15 d in vitro unless otherwise indicated. Either a pool against rat Smaug1 (catalog no. M-086491-00-0010) containing the sequences 5′-AAUAUAAGCUCCUAUCUAC-3′ (siSmaug1*a*), 5′-GACCGGACCUCCACAAUCU-3′ (siSmaug1*b*), 5′-UGGCAGAACUCUCGGGAUU-3′ (siSmaug1*c*), and 5′-ACGCGAAAGUAGAGUAUAU-3′ (siSmaug1*d*) at 25 nM each or the individual sequences at 100 nM were used. A pool of four sequences against rat Smaug2 (siSmaug2, catalog no. M-081919-00) and an siCONTROL nontargeting pool (D-001810-10; Thermo Fisher Scientific) were used at 100 nM.

Drug treatment and neuron stimulation

In all cases, stock solutions were diluted into conditioned medium. Sodium arsenite, used at 1 mM cycloheximide, and puromycin, used at 250 µg/ml, were obtained from Sigma-Aldrich. Emetine, used at 1 µg/ml, was a gift from I.D. Algranatti (Fundación Instituto Leloir, Buenos Aires, Argentina). Hippuristanol was provided by J. Pelletier (McGill University, Montreal, Quebec, Canada) and used at 0.01 mg/ml. Neuron depolarization was induced in 17–20-d cultures by increasing KCl (Sigma-Aldrich) concentration up to 55 mM during 10 min unless otherwise indicated. When indicated, depolarization was performed in the presence of kynurenic acid, used at 4 mM, picrotoxin, AP5, or CNQX (provided by A. Schinder, Fundación Instituto Leloir; and O. Uchitel, University of Buenos Aires, Buenos Aires, Argentina), all used at 50 µM and added 5 min before stimulation. For NMDAR stimulation, 1 µM TTX (Tocris Bioscience) was applied overnight, followed by a five min-pulse with 30 µM NMDA (Sigma-Aldrich) and a variable recovery period in NB. Wortmannin and EGTA-AM (Sigma-Aldrich), used at 20 µM, were added five min before neuron stimulation. KN93, used at 2 µM, and LY294002, used 10 µM, were from Sigma-Aldrich. Stimulation by repeated depolarization was induced as described previously (Wu et al., 2001). In brief, primary hippocampal neurons at 24 d in vitro were treated with 1 µM TTX for 1 d to block spontaneous activity. Then, repeated depolarization stimuli with

90 mM KCl in isotonic Tyrode's solution during 3 min were applied four times with 10 min intervals. TTX was applied during the resting intervals and after the stimulation phase.

FUNCAT

For labeling of newly synthesized proteins, HPG and AHA, both from Invitrogen, were used according to the manufacturer's instructions. Before labeling, neurons were incubated during 30 min in methionine-free DME (Sigma-Aldrich) plus TTX, after an overnight treatment with TTX in NB. Then, HPG was added during 15 min. After a 5-min pulse with NMDA, without any tagged amino acid, and in the absence of methionine and TTX, cells were incubated with AHA during the indicated times. After fixation and permeabilization, cells were incubated with Alexa Fluor 594 azide (Alexa Fluor 594 carboxamido-(6-azidohexanyl) bis(triethylammonium salt); Invitrogen), which reacts with the azide group of AHA-bearing proteins, and then with Alexa Fluor 488 alkyne (Alexa Fluor 488 5-carboxamido-(propargyl), bis(triethylammonium salt)), which reacts with the HPG azide group. Signal intensities were measured in dendrite fragments located at 50 µm or longer distances from the soma to minimize contribution from proteins delivered from the cell body (Dieterich et al., 2010).

IF, FISH, and image analysis

IF of cultured cells was performed after fixation, permeabilization, and blocking as usual (Thomas et al., 2005, 2009; Loschi et al., 2009). Primary antibodies were diluted as follows: anti-mammalian Smaug1, 1:300–1:1,000 (Baez and Boccaccio, 2005); rabbit polyclonal anti-Dcp1 (a gift from J.L. Andersen, University of California, San Diego, La Jolla, CA), 1:100; monoclonal IgG2a anti Dcp1a (Abnova Corporation), 1:1,000; polyclonal rabbit anti-Hedls and anti Rck/p54 (Bethyl Laboratories, Inc.), 1:500; monoclonal IgG2a anti-PSD95 (Millipore), 1:100; IgG2b anti-tubulin βIII and IgG1 anti-MAP2 (both from Sigma-Aldrich), 1:500; IgG1 anti-Synapsin (Synaptic Systems), 1:100; polyclonal anti-Arc (catalog no. 156 003; Synaptic Systems), 1:500; polyclonal anti-Staufen (Thomas et al., 2005), 1:400; IgG2b anti-FMRP, clone 7G1-1 (Developmental Studies Hybridoma Bank), 1:50; IgG1 anti-TIAR (BD), 1:100; and monoclonal anti-CaMKII (Abcam), 1:500. Secondary antibodies coupled to Alexa Fluor 488, Alexa Fluor 555, or Alexa Fluor 666, used at 1:500–1:1,000, were obtained from Invitrogen. Secondary antibodies coupled to Cy2, Cy3, or Cy5, used at 1:300–1:500, were from Jackson ImmunoResearch Laboratories, Inc. Phalloidin conjugated to FITC (Sigma-Aldrich) or to Alexa Fluor 546 (Invitrogen) was used.

Brain sections, provided by A. Schinder and A.J. Ramos (University of Buenos Aires) were stained in a free-floating system, as described previously (Aviles-Reyes et al., 2010). In brief, after antigen retrieval by treatment at 95°C for 5 min, vibratome sections were blocked in 10% normal donkey serum in PBS containing 0.3% Triton X-100, and incubated overnight with anti-Smaug (1:100), anti-synapsin (1:200), or anti-tubulin βIII (1:200) at 4°C. Donkey secondary antibodies anti–rabbit, anti–mouse IgG1, or IgG2b (Jackson) were used at 1:250. Sections were mounted in PVA-Dabco (Sigma-Aldrich).

For FISH, a pBlueScript plasmid (Agilent Technologies) containing 240 bp from the coding region and contiguous 3,280 bp from the 3′ UTR of rat CaMKIIα was provided by S. Kindler (University Medical Center Hamburg-Eppendorf, Hamburg, Germany). Sense and antisense digoxigenin-RNA probes were synthesized according to the manufacturer's instructions (Roche), and combined FISH-IF was performed as described previously (Thomas et al., 2005). In brief, cells were fixed in 4% paraformaldehyde, 4% sucrose, and 2 mM $MgCl_2$ in PBS for 15 min at 37°C; washed three times in 4% sucrose and PBS; and UV cross-linked (CL program, GS Gene Linker; Bio-Rad Laboratories, Inc.). Cells were then treated with 0.3% Triton X-100 in PBS for 5 min, washed with 2 mM $MgCl_2$ in PBS, and dried completely. After prehybridization in 50% formamide, 5× SSC, 0.2% SDS, 50 mg/ml heparin, 250 mg/ml salmon sperm DNA, and 250 mg/ml yeast tRNA (all from Sigma-Aldrich), overnight hybridization was performed at 55°C in the same solution supplemented with 100 mg/ml heparin and 100 ng/ml digoxigenin-riboprobe. After washing twice at room temperature with 1× SSC, 0.1% SDS, and twice at 50°C with 0.2× SSC, 0.1% SDS, blocking was performed with 1% blocking reagent (Boehringer Ingelheim) in PBS. The probe signal was amplified in one or two steps with the following antibodies: biotinylated mouse antidigoxin (Sigma-Aldrich) or sheep antidigoxigenin (Boehringer Ingelheim) followed by biotinylated donkey anti–sheep (Jackson ImmunoResearch Laboratories, Inc.). Then, anti–mouse A488 or streptavidin coupled to Cy2 (Jackson ImmunoResearch Laboratories, Inc.) was used. All incubations were performed for 2 h at room temperature and were followed by three washes in PBS with Tween 20 (PBST). The first antibody for the IF was either included in the antidigoxin antibody solution, or used after the biotinylated donkey anti–sheep. The secondary antibody for IF was always included in the streptavidin mix.

Images were acquired with PASCAL-LSM and LSM510 Meta confocal microscopes (Carl Zeiss), using C-Apochromat 40×/1.2 W Corr or 63×/1.2 W Corr water immersion objectives for the LSM, and an EC "Plan-Neofluor" 40×/1.30 NA oil or Plan-Apochromat 63×/1.4 NA oil objective lenses for the LSM510 Meta. Images were acquired with LSM software (Carl Zeiss), and pixel intensity was always lower that 250, with 255 being the level of saturation. Equipment adjustment was assessed by using 1 µm FocalCheck fluorescent microspheres (Invitrogen). No filters or gamma adjustment were used previous to the analysis of the object's size, number, or intensity with the ImageJ software. The size and number of synapse puncta or Smaug granules was analyzed in maximum-intensity z-stacks of 0.45-µm slices (63×). Values in Fig. 4 A; Fig. 5 (A, B, D, E and F), and Fig. 6 (A–C) are normalized to the number of synapses with S-foci under resting conditions, which were 62% for Fig. 4 A, 75% for Fig. 5 (A, B, and E) and Fig. 6 (A–C), and 67% for Fig. 5 D.

Magnifications in Fig. 1 (A and B), Fig. 2 (A and B), Fig. 3 (A, B, and D), Fig. 7 (A and B), Fig. 8 C, Fig. 9 (C and E), and Fig. 10 A were scaled using bilinear interpolation; and a Gaussian Blur, Sigma radius Max 2 filter, was applied to Fig. 4 A.

Hippocampus fractionation

Hand-dissected hippocampuses from adult mice were fractionated as described previously (Phillips et al., 2001). In brief, a crude synaptosome preparation was extracted in 2% Triton X-100, pH 6, followed by 1% Triton X-100, pH 8.0, to obtain a fraction enriched in soluble presynaptic components, and a fraction containing postsynaptic densities and insoluble presynaptic proteins.

Western blotting and RT-PCR

Western blotting was performed by standard procedures using polyvinylidene fluoride membranes (Immobilon-P polyvinylidene difluoride; Millipore), LumiGlo (Cell Signaling Technology), and Hyperfilm (GE Healthcare). Primary antibodies were used as follows: anti-Smaug1 (Baez and Boccaccio, 2005), diluted 1:5,000–1:10,000; anti–β-actin, 1:5,000–1:10,0000 (Sigma-Aldrich); anti-PSD95 (Millipore), 1:1,000; anti–βIII-tubulin and anti-MAP2 (both from Sigma-Aldrich), 1:5,000; anti-Synapsin (Synaptic Systems), 1:5,000; and anti-Hedls. For semiquantitative analysis, autoradiographs were scanned and signal intensity was assessed with the ImageJ software. RT-PCR was performed as described previously (Baez and Boccaccio, 2005) using the following primers for Smaug1: 5′-TCGACAGCAAAGAAATCGTG-3′ and 5′-AAGGCTGCAAAGTGTCTTGG-3′; and the following primers for β-actin: 5′-TCTGTGTGGATTGGTGGCTCTA-3′ and 5′-CTGCTTGCTGATCCACATCTG-3′.

Statistics

The number of synapses, number cells, and/or dendritic lengths analyzed are indicated in each figure panel. Each experimental point includes duplicate or triplicate coverslips. P-values (*, $P < 0.05$; **, $P < 0.01$; ***, $P < 0.001$) relative to control treatments according to two-way ANOVA or the indicated test were determined using Infostat (Universidad Nacional de Córdoba) or Instat software (GraphPad Software, Inc.). Error bars represent standard error from independent experiments unless otherwise indicated.

Online supplemental material

Fig. S1 shows that a proportion of neuronal S-foci are in contact with PBs under resting conditions and that S-foci localize adjacent to SGs induced in neurons upon exposure to oxidants. Fig. S2 shows that transfected Smaug1-ECFP or ΔSAM-ECFP form foci in cell lines, which are distinct from SGs and in close contact with PBs. Online supplemental material is available at http://www.jcb.org/cgi/content/full/jcb.201108159/DC1.

This paper is dedicated to the memory of Dr. David R. Colman. Dr. Colman died on 1 June 2011.

We are grateful to David R. Colman and Analía Reines (The Montreal Neurological Institute, McGill University, Canada) for training on neuronal culture. We are thankful to Israel Algranati (Instituto Leloir, Arg) for advice on the use of emetine; A. Schinder and Verónica Piatti (Fundación Instituto Leloir); A.J. Ramos and F. Angelo (University of Buenos Aires) for kindly providing tissue section staining and imaging; and A. Schinder and O. Uchitel (Facultad de Ciencias Exactas y Naturales, Universidad de Buenos Aires) for providing knowledge on neuronal stimulation. We are also thankful to M.J. Ortega and M. Neme (Fundación Instituto Leloir) for their assistance in confocal microscopy analysis, and to C.C. Leishman for technical support.

This work was supported by the following grants: UBACyT X834 and UBACyT X311 from University of Buenos Aires, Argentina; PIP 6173 from Consejo Nacional de Investigaciones Científicas y Tecnológicas (CONICET); PICT 38006 and PICT 1965 from Agencia Nacional de Promoción Científica y Tecnológica, (ANPCyT), Argentina, and 1R03TW006037–01A1, National Institutes of Health.

Submitted: 29 August 2011
Accepted: 22 November 2011

References

Aakalu, G., W.B. Smith, N. Nguyen, C. Jiang, and E.M. Schuman. 2001. Dynamic visualization of local protein synthesis in hippocampal neurons. *Neuron*. 30:489–502. http://dx.doi.org/10.1016/S0896-6273(01)00295-1

Anderson, P., and N. Kedersha. 2009. RNA granules: post-transcriptional and epigenetic modulators of gene expression. *Nat. Rev. Mol. Cell Biol.* 10: 430–436. http://dx.doi.org/10.1038/nrm2694

Antar, L.N., R. Afroz, J.B. Dictenberg, R.C. Carroll, and G.J. Bassell. 2004. Metabotropic glutamate receptor activation regulates fragile x mental retardation protein and FMR1 mRNA localization differentially in dendrites and at synapses. *J. Neurosci.* 24:2648–2655. http://dx.doi.org/10.1523/JNEUROSCI.0099-04.2004

Ashraf, S.I., A.L. McLoon, S.M. Sclarsic, and S. Kunes. 2006. Synaptic protein synthesis associated with memory is regulated by the RISC pathway in *Drosophila. Cell*. 124:191–205. http://dx.doi.org/10.1016/j.cell.2005.12.017

Atkins, C.M., N. Nozaki, Y. Shigeri, and T.R. Soderling. 2004. Cytoplasmic polyadenylation element binding protein-dependent protein synthesis is regulated by calcium/calmodulin-dependent protein kinase II. *J. Neurosci.* 24:5193–5201. http://dx.doi.org/10.1523/JNEUROSCI.0854-04.2004

Aviles-Reyes, R.X., M.F. Angelo, A. Villarreal, H. Rios, A. Lazarowski, and A.J. Ramos. 2010. Intermittent hypoxia during sleep induces reactive gliosis and limited neuronal death in rats: implications for sleep apnea. *J. Neurochem.* 112:854–869. http://dx.doi.org/10.1111/j.1471-4159.2009.06535.x

Aviv, T., Z. Lin, S. Lau, L.M. Rendl, F. Sicheri, and C.A. Smibert. 2003. The RNA-binding SAM domain of Smaug defines a new family of post-transcriptional regulators. *Nat. Struct. Biol.* 10:614–621. http://dx.doi.org/10.1038/nsb956

Aviv, T., Z. Lin, G. Ben-Ari, C.A. Smibert, and F. Sicheri. 2006. Sequence-specific recognition of RNA hairpins by the SAM domain of Vts1p. *Nat. Struct. Mol. Biol.* 13:168–176. http://dx.doi.org/10.1038/nsmb1053

Baez, M.V., and G.L. Boccaccio. 2005. Mammalian Smaug is a translational repressor that forms cytoplasmic foci similar to stress granules. *J. Biol. Chem.* 280:43131–43140. http://dx.doi.org/10.1074/jbc.M508374200

Bagni, C., and W.T. Greenough. 2005. From mRNP trafficking to spine dysmorphogenesis: the roots of fragile X syndrome. *Nat. Rev. Neurosci.* 6:376–387. http://dx.doi.org/10.1038/nrn1667

Balagopal, V., and R. Parker. 2009. Polysomes, P bodies and stress granules: states and fates of eukaryotic mRNAs. *Curr. Opin. Cell Biol.* 21:403–408. http://dx.doi.org/10.1016/j.ceb.2009.03.005

Banerjee, S., P. Neveu, and K.S. Kosik. 2009. A coordinated local translational control point at the synapse involving relief from silencing and MOV10 degradation. *Neuron*. 64:871–884. http://dx.doi.org/10.1016/j.neuron.2009.11.023

Banker, G., and K. Goslin. 1998. Culturing Nerve Cells. The MIT Press, Cambridge, MA. 666 pp.

Barbee, S.A., P.S. Estes, A.M. Cziko, J. Hillebrand, R.A. Luedeman, J.M. Coller, N. Johnson, I.C. Howlett, C. Geng, R. Ueda, et al. 2006. Staufen- and FMRP-containing neuronal RNPs are structurally and functionally related to somatic P bodies. *Neuron*. 52:997–1009. http://dx.doi.org/10.1016/j.neuron.2006.10.028

Benoit, B., C.H. He, F. Zhang, S.M. Votruba, W. Tadros, J.T. Westwood, C.A. Smibert, H.D. Lipshitz, and W.E. Theurkauf. 2009. An essential role for the RNA-binding protein Smaug during the *Drosophila* maternal-to-zygotic transition. *Development*. 136:923–932. http://dx.doi.org/10.1242/dev.031815

Bosco, D.A., N. Lemay, H.K. Ko, H. Zhou, C. Burke, T.J. Kwiatkowski Jr., P. Sapp, D. McKenna-Yasek, R.H. Brown Jr., and L.J. Hayward. 2010. Mutant FUS proteins that cause amyotrophic lateral sclerosis incorporate into stress granules. *Hum. Mol. Genet.* 19:4160–4175. http://dx.doi.org/10.1093/hmg/ddq335

Bramham, C.R., and D.G. Wells. 2007. Dendritic mRNA: transport, translation and function. *Nat. Rev. Neurosci.* 8:776–789. http://dx.doi.org/10.1038/nrn2150

Bramham, C.R., P.F. Worley, M.J. Moore, and J.F. Guzowski. 2008. The immediate early gene arc/arg3.1: regulation, mechanisms, and function. *J. Neurosci.* 28:11760–11767. http://dx.doi.org/10.1523/JNEUROSCI.3864-08.2008

Brechbiel, J.L., and E.R. Gavis. 2008. Spatial regulation of nanos is required for its function in dendrite morphogenesis. *Curr. Biol.* 18:745–750. http://dx.doi.org/10.1016/j.cub.2008.04.033

Buchan, J.R., and R. Parker. 2009. Eukaryotic stress granules: the ins and outs of translation. *Mol. Cell*. 36:932–941. http://dx.doi.org/10.1016/j.molcel.2009.11.020

Costa-Mattioli, M., W.S. Sossin, E. Klann, and N. Sonenberg. 2009. Translational control of long-lasting synaptic plasticity and memory. *Neuron*. 61:10–26. http://dx.doi.org/10.1016/j.neuron.2008.10.055

Cougot, N., S.N. Bhattacharyya, L. Tapia-Arancibia, R. Bordonné, W. Filipowicz, E. Bertrand, and F. Rage. 2008. Dendrites of mammalian neurons contain specialized P-body-like structures that respond to neuronal activation. *J. Neurosci.* 28:13793–13804. http://dx.doi.org/10.1523/JNEUROSCI.4155-08.2008

Crucs, S., S. Chatterjee, and E.R. Gavis. 2000. Overlapping but distinct RNA elements control repression and activation of nanos translation. *Mol. Cell*. 5:457–467. http://dx.doi.org/10.1016/S1097-2765(00)80440-2

Dahanukar, A., J.A. Walker, and R.P. Wharton. 1999. Smaug, a novel RNA-binding protein that operates a translational switch in Drosophila. *Mol. Cell*. 4:209–218. http://dx.doi.org/10.1016/S1097-2765(00)80368-8

De Rubeis, S., and C. Bagni. 2010. Fragile X mental retardation protein control of neuronal mRNA metabolism: Insights into mRNA stability. *Mol. Cell. Neurosci.* 43:43–50. http://dx.doi.org/10.1016/j.mcn.2009.09.013

Dictenberg, J.B., S.A. Swanger, L.N. Antar, R.H. Singer, and G.J. Bassell. 2008. A direct role for FMRP in activity-dependent dendritic mRNA transport links filopodial-spine morphogenesis to fragile X syndrome. *Dev. Cell*. 14:926–939. http://dx.doi.org/10.1016/j.devcel.2008.04.003

Didiot, M.C., M. Subramanian, E. Flatter, J.L. Mandel, and H. Moine. 2009. Cells lacking the fragile X mental retardation protein (FMRP) have normal RISC activity but exhibit altered stress granule assembly. *Mol. Biol. Cell*. 20:428–437. http://dx.doi.org/10.1091/mbc.E08-07-0737

Dieterich, D.C., J.J. Hodas, G. Gouzer, I.Y. Shadrin, J.T. Ngo, A. Triller, D.A. Tirrell, and E.M. Schuman. 2010. In situ visualization and dynamics of newly synthesized proteins in rat hippocampal neurons. *Nat. Neurosci.* 13:897–905. http://dx.doi.org/10.1038/nn.2580

di Penta, A., V. Mercaldo, F. Florenzano, S. Munck, M.T. Ciotti, F. Zalfa, D. Mercanti, M. Molinari, C. Bagni, and T. Achsel. 2009. Dendritic LSm1/CBP80-mRNPs mark the early steps of transport commitment and translational control. *J. Cell Biol.* 184:423–435. http://dx.doi.org/10.1083/jcb.200807033

Du, L., and J.D. Richter. 2005. Activity-dependent polyadenylation in neurons. *RNA*. 11:1340–1347. http://dx.doi.org/10.1261/rna.2870505

Dubnau, J., A.S. Chiang, L. Grady, J. Barditch, S. Gossweiler, J. McNeil, P. Smith, F. Buldoc, R. Scott, U. Certa, et al. 2003. The staufen/pumilio pathway is involved in *Drosophila* long-term memory. *Curr. Biol.* 13:286–296. http://dx.doi.org/10.1016/S0960-9822(03)00064-2

Eom, T., L.N. Antar, R.H. Singer, and G.J. Bassell. 2003. Localization of a beta-actin messenger ribonucleoprotein complex with zipcode-binding protein modulates the density of dendritic filopodia and filopodial synapses. *J. Neurosci.* 23:10433–10444.

Eulalio, A., I. Behm-Ansmant, D. Schweizer, and E. Izaurralde. 2007. P-body formation is a consequence, not the cause, of RNA-mediated gene silencing. *Mol. Cell. Biol.* 27:3970–3981. http://dx.doi.org/10.1128/MCB.00128-07

Falley, K., J. Schütt, P. Iglauer, K. Menke, C. Maas, M. Kneussel, S. Kindler, F.S. Wouters, D. Richter, and H.J. Kreienkamp. 2009. Shank1 mRNA: dendritic transport by kinesin and translational control by the 5'untranslated region. *Traffic*. 10:844–857. http://dx.doi.org/10.1111/j.1600-0854.2009.00912.x

Fenger-Grøn, M., C. Fillman, B. Norrild, and J. Lykke-Andersen. 2005. Multiple processing body factors and the ARE binding protein TTP activate mRNA decapping. *Mol. Cell*. 20:905–915. http://dx.doi.org/10.1016/j.molcel.2005.10.031

Ferraiuolo, M.A., S. Basak, J. Dostie, E.L. Murray, D.R. Schoenberg, and N. Sonenberg. 2005. A role for the eIF4E-binding protein 4E-T in P-body formation and mRNA decay. *J. Cell Biol.* 170:913–924. http://dx.doi.org/10.1083/jcb.200504039

Fiore, R., S. Khudayberdiev, M. Christensen, G. Siegel, S.W. Flavell, T.K. Kim, M.E. Greenberg, and G. Schratt. 2009. Mef2-mediated transcription of the miR379-410 cluster regulates activity-dependent dendritogenesis by fine-tuning Pumilio2 protein levels. *EMBO J.* 28:697–710. http://dx.doi.org/10.1038/emboj.2009.10

Foat, B.C., and G.D. Stormo. 2009. Discovering structural cis-regulatory elements by modeling the behaviors of mRNAs. *Mol. Syst. Biol.* 5:268. http://dx.doi.org/10.1038/msb.2009.24

Forrest, K.M., I.E. Clark, R.A. Jain, and E.R. Gavis. 2004. Temporal complexity within a translational control element in the nanos mRNA. *Development*. 131:5849–5857. http://dx.doi.org/10.1242/dev.01460

Franks, T.M., and J. Lykke-Andersen. 2008. The control of mRNA decapping and P-body formation. *Mol. Cell*. 32:605–615. http://dx.doi.org/10.1016/j.molcel.2008.11.001

Fujii, R., S. Okabe, T. Urushido, K. Inoue, A. Yoshimura, T. Tachibana, T. Nishikawa, G.G. Hicks, and T. Takumi. 2005. The RNA binding protein TLS is translocated to dendritic spines by mGluR5 activation and regulates spine morphology. *Curr. Biol.* 15:587–593. http://dx.doi.org/10.1016/j.cub.2005.01.058

Giorgi, C., G.W. Yeo, M.E. Stone, D.B. Katz, C. Burge, G. Turrigiano, and M.J. Moore. 2007. The EJC factor eIF4AIII modulates synaptic strength and neuronal protein expression. *Cell*. 130:179–191. http://dx.doi.org/10.1016/j.cell.2007.05.028

Goetze, B., F. Tuebing, Y. Xie, M.M. Dorostkar, S. Thomas, U. Pehl, S. Boehm, P. Macchi, and M.A. Kiebler. 2006. The brain-specific double-stranded RNA-binding protein Staufen2 is required for dendritic spine morphogenesis. *J. Cell Biol.* 172:221–231. http://dx.doi.org/10.1083/jcb.200509035

Green, J.B., C.D. Gardner, R.P. Wharton, and A.K. Aggarwal. 2003. RNA recognition via the SAM domain of Smaug. *Mol. Cell*. 11:1537–1548. http://dx.doi.org/10.1016/S1097-2765(03)00178-3

Hillebrand, J., K. Pan, A. Kokaram, S. Barbee, R. Parker, and M. Ramaswami. 2010. The Me31B DEAD-Box helicase localizes to postsynaptic foci and regulates expression of a CaMKII reporter mRNA in dendrites of *Drosophila* olfactory projection neurons. *Front Neural Circuits*. 4:121. http://dx.doi.org/10.3389/fncir.2010.00121

Holt, C.E., and S.L. Bullock. 2009. Subcellular mRNA localization in animal cells and why it matters. *Science*. 326:1212–1216. http://dx.doi.org/10.1126/science.1176488

Huang, Y.S., M.Y. Jung, M. Sarkissian, and J.D. Richter. 2002. N-methyl-D-aspartate receptor signaling results in Aurora kinase-catalyzed CPEB phosphorylation and alpha CaMKII mRNA polyadenylation at synapses. *EMBO J.* 21:2139–2148. http://dx.doi.org/10.1093/emboj/21.9.2139

Jeske, M., B. Moritz, A. Anders, and E. Wahle. 2011. Smaug assembles an ATP-dependent stable complex repressing nanos mRNA translation at multiple levels. *EMBO J.* 30:90–103. http://dx.doi.org/10.1038/emboj.2010.283

Johnson, P.E., and L.W. Donaldson. 2006. RNA recognition by the Vts1p SAM domain. *Nat. Struct. Mol. Biol.* 13:177–178. http://dx.doi.org/10.1038/nsmb1039

Kanai, Y., N. Dohmae, and N. Hirokawa. 2004. Kinesin transports RNA: isolation and characterization of an RNA-transporting granule. *Neuron*. 43:513–525. http://dx.doi.org/10.1016/j.neuron.2004.07.022

Kao, D.I., G.M. Aldridge, I.J. Weiler, and W.T. Greenough. 2010. Altered mRNA transport, docking, and protein translation in neurons lacking fragile X mental retardation protein. *Proc. Natl. Acad. Sci. USA*. 107:15601–15606. http://dx.doi.org/10.1073/pnas.1010564107

Kelleher, R.J. III, A. Govindarajan, H.Y. Jung, H. Kang, and S. Tonegawa. 2004. Translational control by MAPK signaling in long-term synaptic plasticity and memory. *Cell*. 116:467–479. http://dx.doi.org/10.1016/S0092-8674(04)00115-1

Kiebler, M.A., and G.J. Bassell. 2006. Neuronal RNA granules: movers and makers. *Neuron*. 51:685–690. http://dx.doi.org/10.1016/j.neuron.2006.08.021

Knowles, R.B., J.H. Sabry, M.E. Martone, T.J. Deerinck, M.H. Ellisman, G.J. Bassell, and K.S. Kosik. 1996. Translocation of RNA granules in living neurons. *J. Neurosci.* 16:7812–7820.

Köhrmann, M., M. Luo, C. Kaether, L. DesGroseillers, C.G. Dotti, and M.A. Kiebler. 1999. Microtubule-dependent recruitment of Staufen-green fluorescent protein into large RNA-containing granules and subsequent dendritic transport in living hippocampal neurons. *Mol. Biol. Cell*. 10:2945–2953.

Kulkarni, M., S. Ozgur, and G. Stoecklin. 2010. On track with P-bodies. *Biochem. Soc. Trans.* 38:242–251. http://dx.doi.org/10.1042/BST0380242

Leski, M.L., and O. Steward. 1996. Protein synthesis within dendrites: ionic and neurotransmitter modulation of synthesis of particular polypeptides characterized by gel electrophoresis. *Neurochem. Res.* 21:681–690. http://dx.doi.org/10.1007/BF02527725

Li, X., G. Quon, H.D. Lipshitz, and Q. Morris. 2010. Predicting in vivo binding sites of RNA-binding proteins using mRNA secondary structure. *RNA*. 16:1096–1107. http://dx.doi.org/10.1261/rna.2017210

Liu-Yesucevitz, L., A. Bilgutay, Y.J. Zhang, T. Vanderweyde, A. Citro, T. Mehta, N. Zaarur, A. McKee, R. Bowser, M. Sherman, et al. 2010. Tar DNA binding protein-43 (TDP-43) associates with stress granules: analysis of cultured cells and pathological brain tissue. *PLoS ONE*. 5:e13250. (published erratum appears in *PLoS ONE*. 2011. 6(9)) http://dx.doi.org/10.1371/journal.pone.0013250

Loschi, M., C.C. Leishman, N. Berardone, and G.L. Boccaccio. 2009. Dynein and kinesin regulate stress-granule and P-body dynamics. *J. Cell Sci.* 122:3973–3982. http://dx.doi.org/10.1242/jcs.051383

Marin, P., K.L. Nastiuk, N. Daniel, J.A. Girault, A.J. Czernik, J. Glowinski, A.C. Nairn, and J. Prémont. 1997. Glutamate-dependent phosphorylation of elongation factor-2 and inhibition of protein synthesis in neurons. *J. Neurosci.* 17:3445–3454.

Martin, K.C., and A. Ephrussi. 2009. mRNA localization: gene expression in the spatial dimension. *Cell*. 136:719–730. http://dx.doi.org/10.1016/j.cell.2009.01.044

Martinez Tosar, L.J., M.G. Thomas, M.V. Baez, I. Ibanez, A. Chernomoretz, and G.L. Boccaccio. 2011. The double-stranded RNA-binding protein staufen. *Front. Biosci.* In press.

Mikl, M., G. Vendra, and M.A. Kiebler. 2011. Independent localization of MAP2, CaMKIIα and β-actin RNAs in low copy numbers. *EMBO Rep.* 12:1077–1084. http://dx.doi.org/10.1038/embor.2011.149

Miller, L.C., V. Blandford, R. McAdam, M.R. Sanchez-Carbente, F. Badeaux, L. DesGroseillers, and W.S. Sossin. 2009. Combinations of DEAD box proteins distinguish distinct types of RNA: protein complexes in neurons. *Mol. Cell. Neurosci.* 40:485–495. http://dx.doi.org/10.1016/j.mcn.2009.01.007

Muddashetty, R.S., S. Kelić, C. Gross, M. Xu, and G.J. Bassell. 2007. Dysregulated metabotropic glutamate receptor-dependent translation of AMPA receptor and postsynaptic density-95 mRNAs at synapses in a mouse model of fragile X syndrome. *J. Neurosci.* 27:5338–5348. http://dx.doi.org/10.1523/JNEUROSCI.0937-07.2007

Nelson, M.R., A.M. Leidal, and C.A. Smibert. 2004. *Drosophila* Cup is an eIF4E-binding protein that functions in Smaug-mediated translational repression. *EMBO J.* 23:150–159. http://dx.doi.org/10.1038/sj.emboj.7600026

Oberstrass, F.C., A. Lee, R. Stefl, M. Janis, G. Chanfreau, and F.H. Allain. 2006. Shape-specific recognition in the structure of the Vts1p SAM domain with RNA. *Nat. Struct. Mol. Biol.* 13:160–167. http://dx.doi.org/10.1038/nsmb1038

Ostroff, L.E., J.C. Fiala, B. Allwardt, and K.M. Harris. 2002. Polyribosomes redistribute from dendritic shafts into spines with enlarged synapses during LTP in developing rat hippocampal slices. *Neuron*. 35:535–545. http://dx.doi.org/10.1016/S0896-6273(02)00785-7

Paradis, S., D.B. Harrar, Y. Lin, A.C. Koon, J.L. Hauser, E.C. Griffith, L. Zhu, L.F. Brass, C. Chen, and M.E. Greenberg. 2007. An RNAi-based approach identifies molecules required for glutamatergic and GABAergic synapse development. *Neuron*. 53:217–232. http://dx.doi.org/10.1016/j.neuron.2006.12.012

Phillips, G.R., J.K. Huang, Y. Wang, H. Tanaka, L. Shapiro, W. Zhang, W.S. Shan, K. Arndt, M. Frank, R.E. Gordon, et al. 2001. The presynaptic particle web: ultrastructure, composition, dissolution, and reconstitution. *Neuron*. 32:63–77. http://dx.doi.org/10.1016/S0896-6273(01)00450-0

Pi, H.J., N. Otmakhov, F. El Gaamouch, D. Lemelin, P. De Koninck, and J. Lisman. 2010. CaMKII control of spine size and synaptic strength: role of phosphorylation states and nonenzymatic action. *Proc. Natl. Acad. Sci. USA*. 107:14437–14442. http://dx.doi.org/10.1073/pnas.1009268107

Poon, M.M., S.H. Choi, C.A. Jamieson, D.H. Geschwind, and K.C. Martin. 2006. Identification of process-localized mRNAs from cultured rodent hippocampal neurons. *J. Neurosci.* 26:13390–13399. http://dx.doi.org/10.1523/JNEUROSCI.3432-06.2006

Ravindranathan, S., F.C. Oberstrass, and F.H. Allain. 2010. Increase in backbone mobility of the VTS1p-SAM domain on binding to SRE-RNA. *J. Mol. Biol.* 396:732–746. http://dx.doi.org/10.1016/j.jmb.2009.12.004

Rendl, L.M., M.A. Bieman, and C.A. Smibert. 2008. *S. cerevisiae* Vts1p induces deadenylation-dependent transcript degradation and interacts with the Ccr4p-Pop2p-Not deadenylase complex. *RNA*. 14:1328–1336. http://dx.doi.org/10.1261/rna.955508

Rouget, C., C. Papin, A. Boureux, A.C. Meunier, B. Franco, N. Robine, E.C. Lai, A. Pelisson, and M. Simonelig. 2010. Maternal mRNA deadenylation and decay by the piRNA pathway in the early *Drosophila* embryo. *Nature*. 467:1128–1132. http://dx.doi.org/10.1038/nature09465

Salazar, A.M., E.J. Silverman, K.P. Menon, and K. Zinn. 2010. Regulation of synaptic Pumilio function by an aggregation-prone domain. *J. Neurosci.* 30:515–522. http://dx.doi.org/10.1523/JNEUROSCI.2523-09.2010

Savas, J.N., A. Makusky, S. Ottosen, D. Baillat, F. Then, D. Krainc, R. Shiekhattar, S.P. Markey, and N. Tanese. 2008. Huntington's disease protein contributes to RNA-mediated gene silencing through association with Argonaute and P bodies. *Proc. Natl. Acad. Sci. USA*. 105:10820–10825. http://dx.doi.org/10.1073/pnas.0800658105

Scheetz, A.J., A.C. Nairn, and M. Constantine-Paton. 2000. NMDA receptor-mediated control of protein synthesis at developing synapses. *Nat. Neurosci.* 3:211–216. http://dx.doi.org/10.1038/72915

Schratt, G.M., F. Tuebing, E.A. Nigh, C.G. Kane, M.E. Sabatini, M. Kiebler, and M.E. Greenberg. 2006. A brain-specific microRNA regulates dendritic spine development. *Nature*. 439:283–289. http://dx.doi.org/10.1038/nature04367

Schuman, E.M., J.L. Dynes, and O. Steward. 2006. Synaptic regulation of translation of dendritic mRNAs. *J. Neurosci.* 26:7143–7146. http://dx.doi.org/10.1523/JNEUROSCI.1796-06.2006

Semotok, J.L., R.L. Cooperstock, B.D. Pinder, H.K. Vari, H.D. Lipshitz, and C.A. Smibert. 2005. Smaug recruits the CCR4/POP2/NOT deadenylase complex to trigger maternal transcript localization in the early *Drosophila* embryo. *Curr. Biol.* 15:284–294. http://dx.doi.org/10.1016/j.cub.2005.01.048

Semotok, J.L., H. Luo, R.L. Cooperstock, A. Karaiskakis, H.K. Vari, C.A. Smibert, and H.D. Lipshitz. 2008. *Drosophila* maternal Hsp83 mRNA destabilization is directed by multiple SMAUG recognition elements in the open reading frame. *Mol. Cell. Biol.* 28:6757–6772. http://dx.doi.org/10.1128/MCB.00037-08

Shiina, N., K. Shinkura, and M. Tokunaga. 2005. A novel RNA-binding protein in neuronal RNA granules: regulatory machinery for local translation. *J. Neurosci.* 25:4420–4434. http://dx.doi.org/10.1523/JNEUROSCI.0382-05.2005

Shiina, N., K. Yamaguchi, and M. Tokunaga. 2010. RNG105 deficiency impairs the dendritic localization of mRNAs for Na+/K+ ATPase subunit isoforms and leads to the degeneration of neuronal networks. *J. Neurosci.* 30:12816–12830. http://dx.doi.org/10.1523/JNEUROSCI.6386-09.2010

Smibert, C.A., J.E. Wilson, K. Kerr, and P.M. Macdonald. 1996. smaug protein represses translation of unlocalized nanos mRNA in the *Drosophila* embryo. *Genes Dev.* 10:2600–2609. http://dx.doi.org/10.1101/gad.10.20.2600

Smibert, C.A., Y.S. Lie, W. Shillinglaw, W.J. Henzel, and P.M. Macdonald. 1999. Smaug, a novel and conserved protein, contributes to repression of nanos mRNA translation in vitro. *RNA*. 5:1535–1547. http://dx.doi.org/10.1017/S1355838299991392

Steward, O., and P.F. Worley. 2001. A cellular mechanism for targeting newly synthesized mRNAs to synaptic sites on dendrites. *Proc. Natl. Acad. Sci. USA*. 98:7062–7068. http://dx.doi.org/10.1073/pnas.131146398

Steward, O., C.S. Wallace, G.L. Lyford, and P.F. Worley. 1998. Synaptic activation causes the mRNA for the IEG Arc to localize selectively near activated postsynaptic sites on dendrites. *Neuron*. 21:741–751. http://dx.doi.org/10.1016/S0896-6273(00)80591-7

Sutton, M.A., and E.M. Schuman. 2006. Dendritic protein synthesis, synaptic plasticity, and memory. *Cell*. 127:49–58. http://dx.doi.org/10.1016/j.cell.2006.09.014

Sutton, M.A., N.R. Wall, G.N. Aakalu, and E.M. Schuman. 2004. Regulation of dendritic protein synthesis by miniature synaptic events. *Science*. 304:1979–1983. http://dx.doi.org/10.1126/science.1096202

Sutton, M.A., H.T. Ito, P. Cressy, C. Kempf, J.C. Woo, and E.M. Schuman. 2006. Miniature neurotransmission stabilizes synaptic function via tonic suppression of local dendritic protein synthesis. *Cell*. 125:785–799. http://dx.doi.org/10.1016/j.cell.2006.03.040

Sutton, M.A., A.M. Taylor, H.T. Ito, A. Pham, and E.M. Schuman. 2007. Postsynaptic decoding of neural activity: eEF2 as a biochemical sensor coupling miniature synaptic transmission to local protein synthesis. *Neuron*. 55:648–661. http://dx.doi.org/10.1016/j.neuron.2007.07.030

Tadros, W., A.L. Goldman, T. Babak, F. Menzies, L. Vardy, T. Orr-Weaver, T.R. Hughes, J.T. Westwood, C.A. Smibert, and H.D. Lipshitz. 2007. SMAUG is a major regulator of maternal mRNA destabilization in *Drosophila* and its translation is activated by the PAN GU kinase. *Dev. Cell*. 12:143–155. http://dx.doi.org/10.1016/j.devcel.2006.10.005

Thomas, M.G., L.J. Martinez Tosar, M. Loschi, J.M. Pasquini, J. Correale, S. Kindler, and G.L. Boccaccio. 2005. Staufen recruitment into stress granules does not affect early mRNA transport in oligodendrocytes. *Mol. Biol. Cell*. 16:405–420. http://dx.doi.org/10.1091/mbc.E04-06-0516

Thomas, M.G., L.J. Martinez Tosar, M.A. Desbats, C.C. Leishman, and G.L. Boccaccio. 2009. Mammalian Staufen 1 is recruited to stress granules and impairs their assembly. *J. Cell Sci.* 122:563–573. http://dx.doi.org/10.1242/jcs.038208

Thomas, M.G., M. Loschi, M.A. Desbats, and G.L. Boccaccio. 2011. RNA granules: the good, the bad and the ugly. *Cell. Signal.* 23:324–334. http://dx.doi.org/10.1016/j.cellsig.2010.08.011

Vessey, J.P., A. Vaccani, Y. Xie, R. Dahm, D. Karra, M.A. Kiebler, and P. Macchi. 2006. Dendritic localization of the translational repressor Pumilio 2 and its contribution to dendritic stress granules. *J. Neurosci.* 26:6496–6508. http://dx.doi.org/10.1523/JNEUROSCI.0649-06.2006

Vessey, J.P., P. Macchi, J.M. Stein, M. Mikl, K.N. Hawker, P. Vogelsang, K. Wieczorek, G. Vendra, J. Riefler, F. Tübing, et al. 2008. A loss of function allele for murine Staufen1 leads to impairment of dendritic Staufen1-RNP delivery and dendritic spine morphogenesis. *Proc. Natl. Acad. Sci. USA*. 105:16374–16379. http://dx.doi.org/10.1073/pnas.0804583105

Vessey, J.P., L. Schoderboeck, E. Gingl, E. Luzi, J. Riefler, F. Di Leva, D. Karra, S. Thomas, M.A. Kiebler, and P. Macchi. 2010. Mammalian Pumilio 2 regulates dendrite morphogenesis and synaptic function. *Proc. Natl. Acad. Sci. USA*. 107:3222–3227. http://dx.doi.org/10.1073/pnas.0907128107

Wang, I.F., L.S. Wu, H.Y. Chang, and C.K. Shen. 2008. TDP-43, the signature protein of FTLD-U, is a neuronal activity-responsive factor. *J. Neurochem.* 105:797–806. http://dx.doi.org/10.1111/j.1471-4159.2007.05190.x

Wilczynska, A., C. Aigueperse, M. Kress, F. Dautry, and D. Weil. 2005. The translational regulator CPEB1 provides a link between dcp1 bodies and stress granules. *J. Cell Sci.* 118:981–992. http://dx.doi.org/10.1242/jcs.01692

Wu, L., D. Wells, J. Tay, D. Mendis, M.A. Abbott, A. Barnitt, E. Quinlan, A. Heynen, J.R. Fallon, and J.D. Richter. 1998. CPEB-mediated cytoplasmic polyadenylation and the regulation of experience-dependent translation of alpha-CaMKII mRNA at synapses. *Neuron*. 21:1129–1139. http://dx.doi.org/10.1016/S0896-6273(00)80630-3

Wu, G.Y., K. Deisseroth, and R.W. Tsien. 2001. Spaced stimuli stabilize MAPK pathway activation and its effects on dendritic morphology. *Nat. Neurosci.* 4:151–158. http://dx.doi.org/10.1038/83976

Wu, K.Y., U. Hengst, L.J. Cox, E.Z. Macosko, A. Jeromin, E.R. Urquhart, and S.R. Jaffrey. 2005. Local translation of RhoA regulates growth cone collapse. *Nature*. 436:1020–1024. http://dx.doi.org/10.1038/nature03885

Zaessinger, S., I. Busseau, and M. Simonelig. 2006. Oskar allows nanos mRNA translation in *Drosophila* embryos by preventing its deadenylation by Smaug/CCR4. *Development*. 133:4573–4583. http://dx.doi.org/10.1242/dev.02649

Zalfa, F., M. Giorgi, B. Primerano, A. Moro, A. Di Penta, S. Reis, B. Oostra, and C. Bagni. 2003. The fragile X syndrome protein FMRP associates with BC1 RNA and regulates the translation of specific mRNAs at synapses. *Cell*. 112:317–327. http://dx.doi.org/10.1016/S0092-8674(03)00079-5

Zalfa, F., T. Achsel, and C. Bagni. 2006. mRNPs, polysomes or granules: FMRP in neuronal protein synthesis. *Curr. Opin. Neurobiol.* 16:265–269. http://dx.doi.org/10.1016/j.conb.2006.05.010

Zalfa, F., B. Eleuteri, K.S. Dickson, V. Mercaldo, S. De Rubeis, A. di Penta, E. Tabolacci, P. Chiurazzi, G. Neri, S.G. Grant, and C. Bagni. 2007. A new function for the fragile X mental retardation protein in regulation of PSD-95 mRNA stability. *Nat. Neurosci.* 10:578–587. http://dx.doi.org/10.1038/nn1893

Zeitelhofer, M., D. Karra, P. Macchi, M. Tolino, S. Thomas, M. Schwarz, M. Kiebler, and R. Dahm. 2008. Dynamic interaction between P-bodies and transport ribonucleoprotein particles in dendrites of mature hippocampal neurons. *J. Neurosci.* 28:7555–7562. http://dx.doi.org/10.1523/JNEUROSCI.0104-08.2008